

Supporting Information

Electrophilic Phenoxy-substituted Phosphonium Cations

James H. W. LaFortune, Timothy C. Johnstone, Manuel Pérez, Daniel Winkelhaus, Vitali Podgorny and Douglas W. Stephan *

This PDF file includes:

1. Materials and Methods.....	3
2. Synthesis of Catalysts	5
2.1 [(PhO)P(C ₆ F ₅) ₃][B(C ₆ F ₅) ₄] (1)	5
2.2 [(p-FPhO)P(C ₆ F ₅) ₃][B(C ₆ F ₅) ₄] (2)	8
2.3 [(2,4-F ₂ PhO)P(C ₆ F ₅) ₃][B(C ₆ F ₅) ₄] (3)	10
2.4 [(C ₆ F ₅ O)P(C ₆ F ₅) ₃][B(C ₆ F ₅) ₄] (4)	13
2.5 [(HO)P(C ₆ F ₅) ₃][B(C ₆ F ₅) ₄] (5)	15
3. Gutmann-Beckett Test	17
4. Air Stability Test.....	21
4.1 Air Stability of Cations 1-4	21
4.2 Identification of Decomposition Product of 1-4	23
4.3 Air Stability of [FP(C ₆ F ₅) ₃][B(C ₆ F ₅) ₄] and Decomposition Product Identification.....	24
5. Lewis Acid Catalysis	25
5.1 Dimerization of 1,1-diphenylethylene	25
5.2 Hydrodefluorination of 1-fluoroadamantane.....	27
5.3 Hydrosilylation of α -methylstyrene	29
5.4 Dehydrocoupling of phenol with Et ₃ SiH	32
5.5 Hydrodeoxygenation of benzophenone	35
6. Computational Details	37

1. Materials and Methods

General Remarks

All manipulations were performed in a MB Unilab glove box produced by MBraun or using standard Schlenk techniques under an inert atmosphere of anhydrous N₂. All glassware was oven-dried and cooled under vacuum before use. Dry, oxygen-free solvents (dichloromethane, tetrahydrofuran, cyclohexane, and *n*-pentane) were prepared using an Innovative Technologies solvent purification system or deoxygenated and distilled over sodium benzophenone. CD₂Cl₂ (Aldrich) was deoxygenated, distilled over CaH₂, then stored over 3 Å molecular sieves before use. Commercial reagents were purchased from Sigma-Aldrich, Strem Chemicals, TCI Chemicals or Alfa Aesar, and were used without further purification unless indicated otherwise. [Et₃SiOPh_xF_{5-x}]^[1], [FP(C₆F₅)₃][B(C₆F₅)₄]^[2], [CIP(C₆F₅)₃][B(C₆F₅)₄]^[3], [H(OEt₂)₂][B(C₆F₅)₄]^[4], OP(C₆F₅)₃^[5] and NaOC₆F₅^[6] were prepared according to literature procedures. NMR spectra were obtained on an Agilent DD2-700 MHz, an Agilent DD2-500 MHz, a Bruker AvancellII-400 MHz or a Varian Mercury-300 MHz spectrometer. ¹H, ¹³C{¹H}, ³¹P{¹H}, ¹⁹F, and ¹¹B{¹H} NMR chemical shifts (δ/ppm) are referenced to Me₄Si, Me₄Si, H₃PO₄, CFCl₃, and BF₃•OEt₂, respectively. Assignments of individual resonances were performed using 2D NMR techniques (HMBC, HSQC, HH-COSY) when necessary. High-resolution mass spectra (HRMS) were obtained on an Agilent 6538 Q-TOF (ESI), a GCT Premier (EI), or a JEOL AccuTOF (DART) mass spectrometer. Elemental analyses were performed at the University of Toronto employing a Perkin Elmer 2400 Series II CHNS Analyser. In the case of **1-3**, repeated attempts to obtain satisfactory C analyses gave consistently low values. This was attributable to incomplete combustion and the formation of boron carbide.

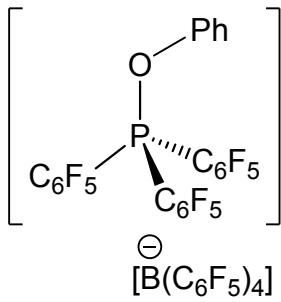
X-ray Diffraction Studies

Single crystals were coated with paratone oil, mounted on a cryoloop and frozen under a stream of cold nitrogen. Data were collected on a Bruker Apex2 X-ray diffractometer at 150 (2) K for all crystals using graphite monochromated Mo-Kα radiation (0.71073 Å). Data were collected using Bruker APEX-2 software and processed using SHELX and an absorption correction applied using multi-scan within the APEX-2 program. All structures were solved and refined by direct methods

within the SHELXTL package. These data can be obtained free of charge from the Cambridge Crystallographic Data Centre.

2. Synthesis of Catalysts

2.1 $[(PhO)P(C_6F_5)_3][B(C_6F_5)_4]$ (1)



⊕ To a solution of $[\text{FP}(\text{C}_6\text{F}_5)_3][\text{B}(\text{C}_6\text{F}_5)_4]$ (74 mg, 0.06 mmol) in CH_2Cl_2 (5 mL) was added triethyl(phenoxy)silane (PhOSiEt_3 , 63 mg, 0.3 mmol). The reaction mixture was left for 2 h at room temperature, which yielded a tan coloured solution. The solvent was removed *in vacuo* yielding a tan coloured solid which was then washed with *n*-pentane (3 x 3 mL). The solid was then re-dissolved in CH_2Cl_2 (3 mL), layered with cyclohexane (12 mL), and left overnight to recrystallize. After decanting the supernatant, the solid was dried *in vacuo* to afford a white powder (49 mg, 67% yield). ^1H NMR (500 MHz, CD_2Cl_2): $\delta = 7.04$ (m, 2H; *m*-Ph), 7.48 ppm (m, 3H; *o*-Ph and *p*-Ph). $^{11}\text{B}\{^1\text{H}\}$ NMR (192 Hz, CD_2Cl_2): $\delta = -16.7$ ppm (s). ^{19}F NMR (564 MHz, CD_2Cl_2): $\delta = -125.5$ (t, $^3J_{\text{FF}} = 14$ Hz, 6F; $\text{P}(\text{o-C}_6\text{F}_5)_3$) -126.9 (sept, $^3J_{\text{FF}} = 10$ Hz, 3F; $\text{P}(\text{p-C}_6\text{F}_5)_3$), -133.4 (s(br), 8F; $\text{B}(\text{o-C}_6\text{F}_5)_4$), -151.3 (m, 6F; $\text{P}(\text{m-C}_6\text{F}_5)_3$), -164.0 (t, $^3J_{\text{FF}} = 20$ Hz, 4F; $\text{B}(\text{p-C}_6\text{F}_5)_4$), -167.9 ppm (m(br), 8F; $\text{B}(\text{m-C}_6\text{F}_5)_4$). $^{31}\text{P}\{^1\text{H}\}$ NMR (243 MHz, CD_2Cl_2): $\delta = 36.8$ ppm (s). $^{13}\text{C}\{^1\text{H}\}$ NMR (125 MHz, CD_2Cl_2): $\delta = 119.2$ (d, $^3J_{\text{PC}} = 5$ Hz, 2C; *o*-Ph), 130.2 (d, $^4J_{\text{PC}} = 2$ Hz, 2C; *p*-Ph), 132.4 (d, $^4J_{\text{PC}} = 2$ Hz, 2C; *m*-Ph), 136.2 (d(br), $^1J_{\text{FC}} = 345$ Hz, 8C; $\text{B}(\text{o-C}_6\text{F}_5)_4$), 138.1 (d(br), $^1J_{\text{FC}} = 345$ Hz, 4C; $\text{B}(\text{p-C}_6\text{F}_5)_4$), 139.0 (d(br), $^1J_{\text{FC}} = 380$ Hz, 6C; $\text{P}(\text{o-C}_6\text{F}_5)_3$), 148.1 (d(br), $^1J_{\text{FC}} = 345$ Hz, 8C; $\text{B}(\text{m-C}_6\text{F}_5)_4$), 148.2 (d(br), $^1J_{\text{FC}} = 380$ Hz, 6C; $\text{P}(\text{p-C}_6\text{F}_5)_3$), 149.6 ppm (d(br), $^1J_{\text{FC}} = 380$ Hz, 3C; $\text{P}(\text{p-C}_6\text{F}_5)_3$), resonance for *ipso*-carbons was not observed. HRMS (TOF MS EI+): m/z 624.9815 (calcd. for $[(\text{PhO})\text{P}(\text{C}_6\text{F}_5)_3]^+$: 624.9839); elemental analysis calcd (%) for $\text{C}_{48}\text{H}_5\text{BF}_{35}\text{OP}$: C, 44.20; H, 0.39; found: C, 42.86; H, 0.38.

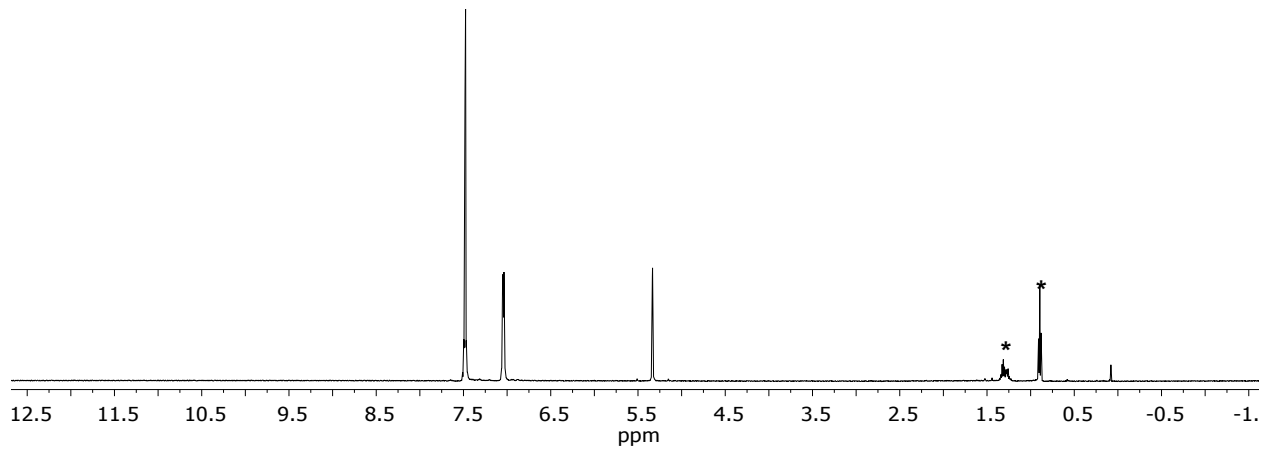


Figure 1. ^1H (CD_2Cl_2) NMR spectrum. Asterisks denote solvent impurities.

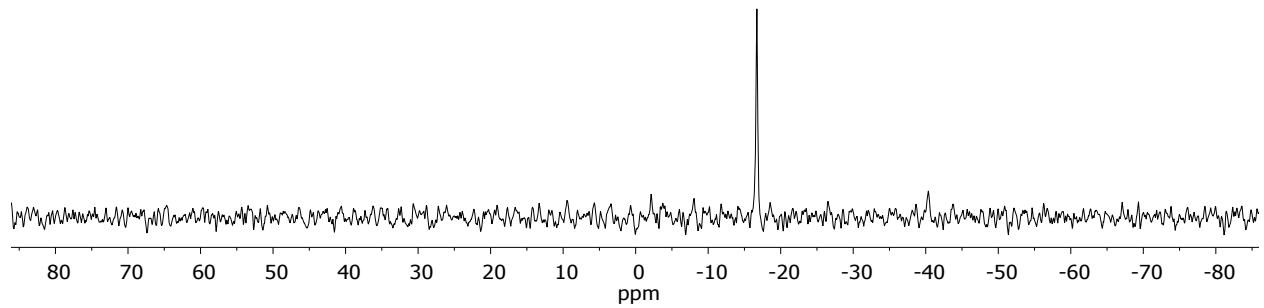


Figure 2. $^{11}\text{B}\{^1\text{H}\}$ (CD_2Cl_2) NMR spectrum.

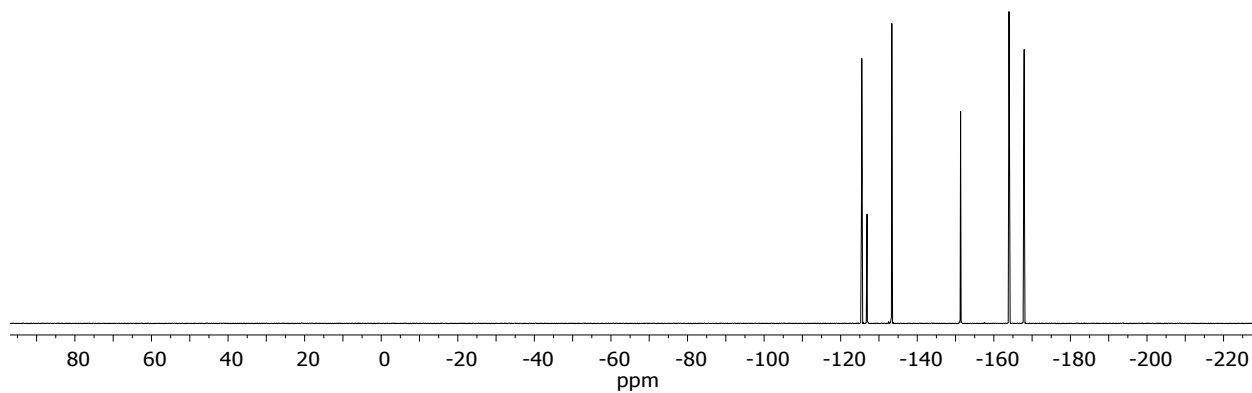


Figure 3. ^{19}F (CD_2Cl_2) NMR spectrum.

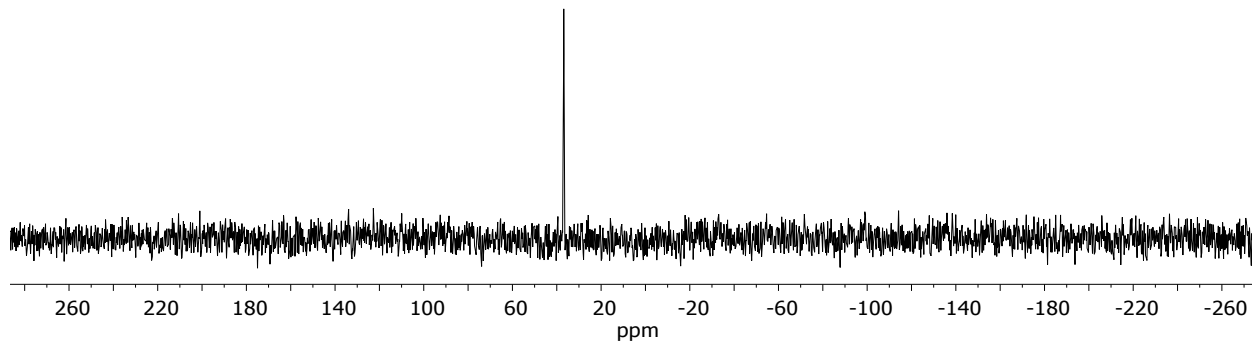


Figure 4. $^{31}\text{P}\{^1\text{H}\}$ (CD_2Cl_2) NMR spectrum.

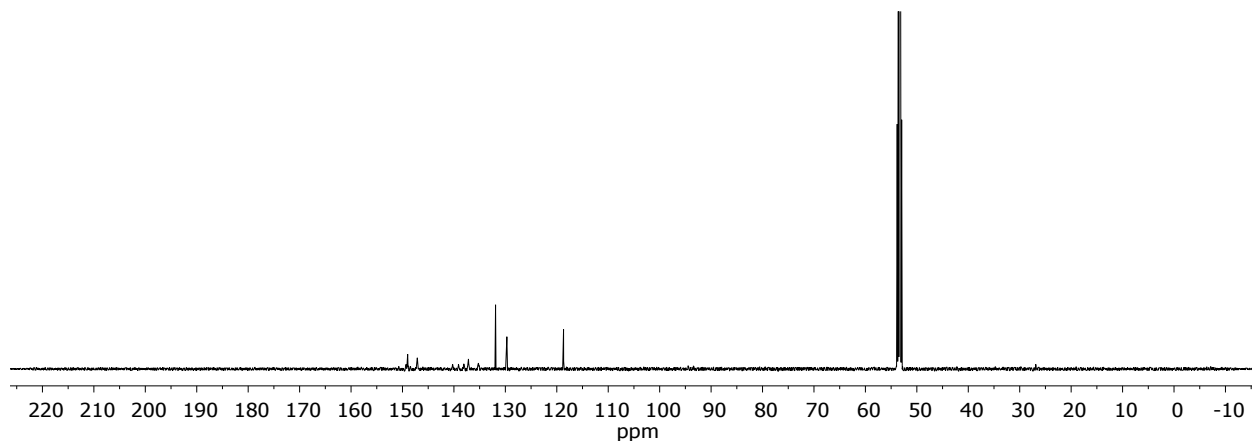
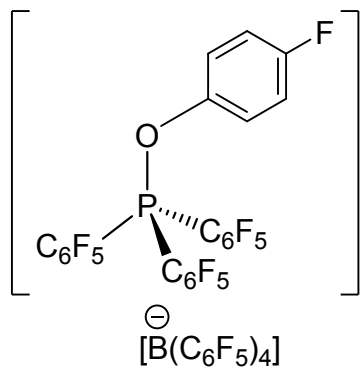


Figure 5. $^{13}\text{C}\{^1\text{H}\}$ (CD_2Cl_2) NMR spectrum.

2.2 $[(p\text{-}FPhO)P(C_6F_5)_3][B(C_6F_5)_4]$ (2)



To a solution of $[\text{FP}(\text{C}_6\text{F}_5)_3][\text{B}(\text{C}_6\text{F}_5)_4]$ (74 mg, 0.06 mmol) in CH_2Cl_2 (5 mL) was added triethyl(*para*-fluorophenoxy)-silane (*p*- FPhOSiEt_3 , 68 mg, 0.3 mmol). The reaction mixture was heated to 60°C for 24 h, which yielded a tan coloured solution. The solvent was removed *in vacuo* yielding a tan coloured solid which was then washed with *n*-pentane (3 x 3 mL). The solid was then re-dissolved in CH_2Cl_2 (3 mL), layered with cyclohexane (12 mL),

and left overnight to recrystallize. After decanting the supernatant, the solid was dried *in vacuo* to afford a white powder (69 mg, 94% yield). ^1H NMR (400 MHz, CD_2Cl_2): δ = 7.05 (m, 2H; *o*- $\text{C}_6\text{H}_4\text{F}$), 7.18 ppm (m, 2H; *m*- $\text{C}_6\text{H}_4\text{F}$). $^{11}\text{B}\{\text{H}\}$ NMR (160 MHz, CD_2Cl_2): δ = -16.7 ppm (s). ^{19}F NMR (470 MHz, CD_2Cl_2): δ = -109.5 (m, 1F; *p*- $\text{C}_6\text{H}_4\text{F}$), -125.5 (t, $^3J_{\text{FF}} = 14$ Hz, 6F; $\text{P}(\text{o-C}_6\text{F}_5)$), -126.3 (sept, $^3J_{\text{FF}} = 10$ Hz, 3F; $\text{P}(\text{p-C}_6\text{F}_5)$), -133.4 (s(br), 8F; $\text{B}(\text{o-C}_6\text{F}_5)_4$), -151.0 (m, 6F; $\text{P}(\text{m-C}_6\text{F}_5)$), -163.9 (t, $^3J_{\text{FF}} = 20$ Hz, 4F; $\text{B}(\text{p-C}_6\text{F}_5)_4$), -167.9 ppm (m(br), 8F; $\text{B}(\text{m-C}_6\text{F}_5)_4$). $^{31}\text{P}\{\text{H}\}$ NMR (202 MHz, CD_2Cl_2): δ = 37.7 ppm (s). $^{13}\text{C}\{\text{H}\}$ NMR (125 MHz, CD_2Cl_2): δ = 119.3 (d, $^3J_{\text{FC}} = 25$ Hz, 2C; *m*- $\text{C}_6\text{H}_4\text{F}$), 121.1 (s(br), 2C; *o*- $\text{C}_6\text{H}_4\text{F}$), 136.2 (d(br), $^1J_{\text{FC}} = 345$ Hz, 8C; $\text{B}(\text{o-C}_6\text{F}_5)_4$), 138.2 (d(br), $^1J_{\text{FC}} = 345$ Hz, 4C; $\text{B}(\text{p-C}_6\text{F}_5)_4$), 139.2 (d(br), $^1J_{\text{FC}} = 380$ Hz, 6C; $\text{P}(\text{o-C}_6\text{F}_5)_3$), 148.0 (d(br), $^1J_{\text{FC}} = 345$ Hz, 8C; $\text{B}(\text{m-C}_6\text{F}_5)_4$), 148.3 (d(br), $^1J_{\text{FC}} = 380$ Hz, 6C; $\text{P}(\text{m-C}_6\text{F}_5)_3$), 149.7 ppm (d(br), $^1J_{\text{FC}} = 345$ Hz, 3C; $\text{P}(\text{p-C}_6\text{F}_5)_3$), resonances for *ipso*-carbons and *p*- FC_6H_4 carbon were not observed. HRMS (TOF-MS E \ddagger I+): m/z 642.9744 (calcd. for $[(p\text{-}FPhO)P(\text{C}_6\text{F}_5)_3]^+$: 642.9721). HRMS (TOF- MS E \ddagger I+) of decomposition product: m/z 54895255 (calcd. for $[(\text{HO})\text{P}(\text{C}_6\text{F}_5)_3]^+$: 54895156); elemental analysis calcd (%) for $\text{C}_{48}\text{H}_4\text{BF}_{36}\text{OP}$: C, 43.60; H, 0.30; found: C, 41.58; H, 0.26.

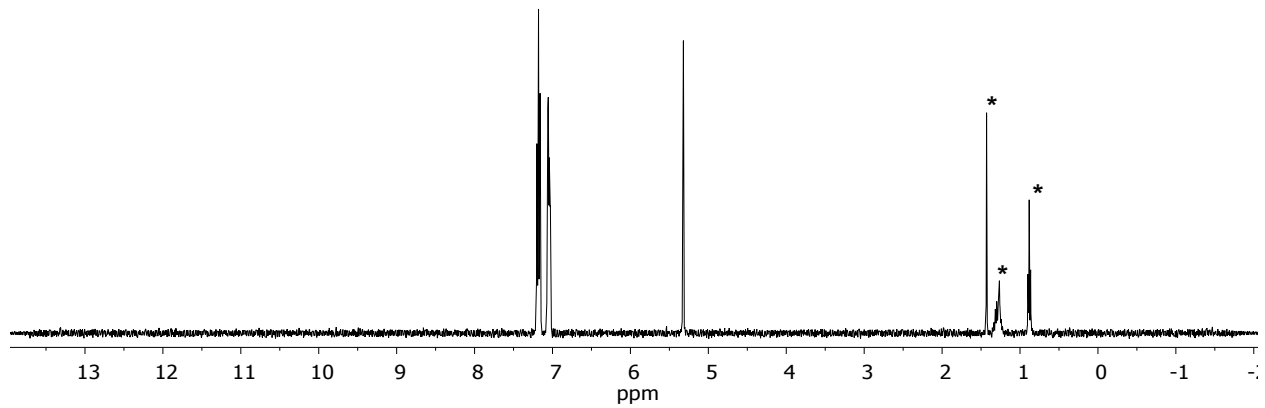


Figure 6. ${}^1\text{H}$ (CD_2Cl_2) NMR spectrum. Asterisks denote solvent impurities.

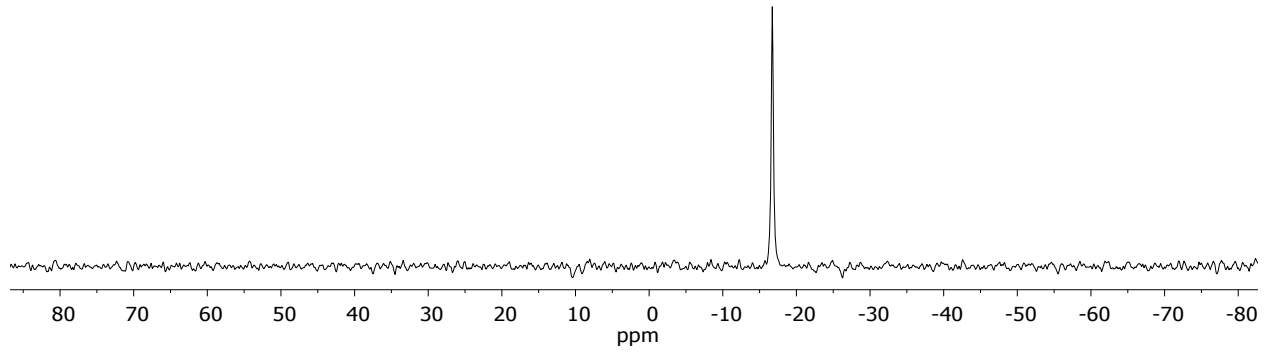


Figure 7. ${}^{11}\text{B}\{{}^1\text{H}\}$ (CD_2Cl_2) NMR spectrum.

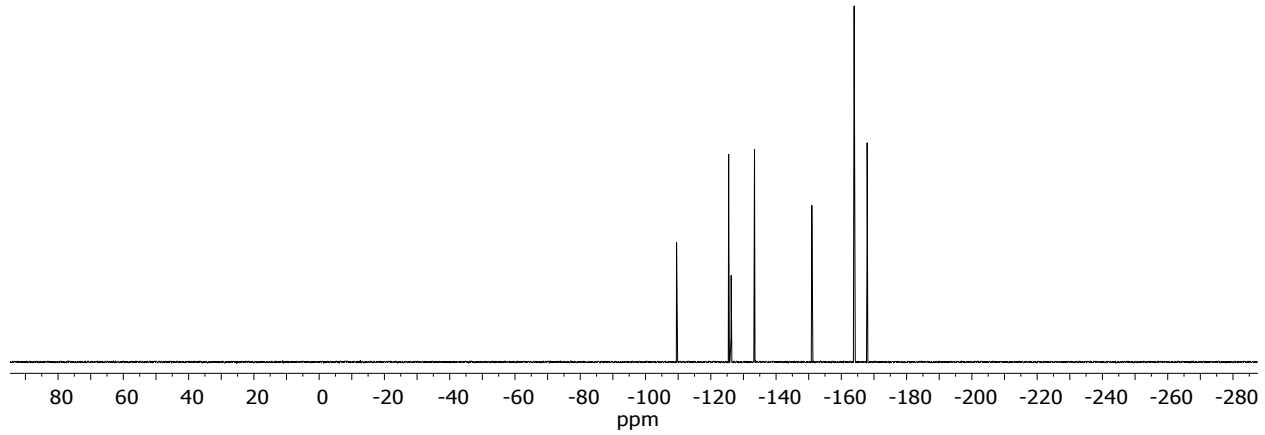


Figure 8. ${}^{19}\text{F}$ (CD_2Cl_2) NMR spectrum.

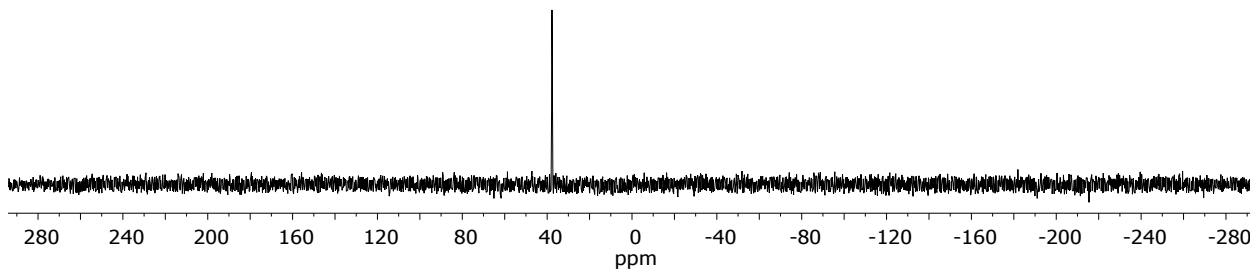


Figure 9. $^{13}\text{P}\{^1\text{H}\}$ (CD_2Cl_2) NMR spectrum.

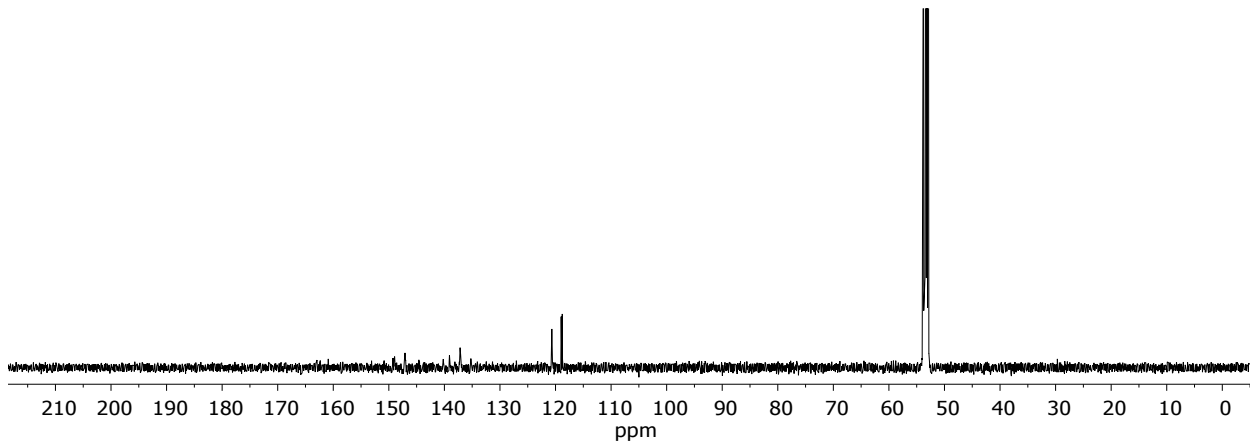
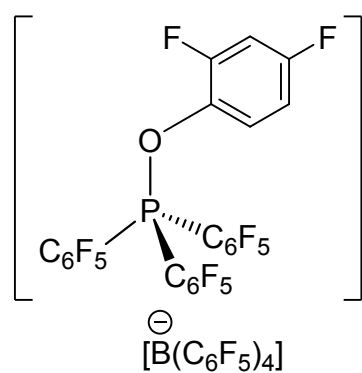


Figure 10. $^{13}\text{C}\{^1\text{H}\}$ (CD_2Cl_2) NMR spectrum.

2.3 $[(2,4\text{-F}_2\text{PhO})\text{P}(\text{C}_6\text{F}_5)_3][\text{B}(\text{C}_6\text{F}_5)_4]$ (3)



To a solution of $[\text{FP}(\text{C}_6\text{F}_5)_3][\text{B}(\text{C}_6\text{F}_5)_4]$ (74 mg, 0.06 mmol) in CH_2Cl_2 (8 mL) was added triethyl(2,4-difluorophenoxy)-silane (2,4- $\text{F}_2\text{PhOSiEt}_3$, 73 mg, 0.3 mmol). The reaction mixture was transferred into a 50 mL Schlenk flask, attached to a Schlenk line, and heated to 60 °C for 48 h, yielding a tan coloured solution. The reaction vessel was returned dry box and the solution transferred to a 20 mL vial. The solvent was removed *in vacuo*

and the solid residue was washed with *n*-pentane (3 x 3 mL). The solid was then re-dissolved in CH_2Cl_2 (3 mL), layered with cyclohexane (12 mL), and left overnight to recrystallize. After

decanting the supernatant, the solid was dried *in vacuo* to afford a white powder (72 mg, 91% yield). ^1H NMR (500 MHz, CD_2Cl_2): δ = 7.08 (m, 2H; 3- $\text{C}_6\text{F}_2\text{H}_3$, 5- $\text{C}_6\text{F}_2\text{H}_3$), 7.37 ppm (dddd, $^3J_{\text{FH}} = 9$ Hz, $^3J_{\text{HH}} = 9$ Hz, $^4J_{\text{HH}} = 5$ Hz, $^5J_{\text{FH}} = 2$ Hz; 1H; 6- $\text{C}_6\text{F}_2\text{H}_3$). $^{11}\text{B}\{\text{H}\}$ NMR (160 MHz, CD_2Cl_2): δ = -16.7 ppm (s). ^{19}F NMR (470 MHz, CD_2Cl_2): δ = -104.5 (m, 1F; *p*- $\text{C}_6\text{F}_2\text{H}_3$), -124.4 (s(br), 1F; *o*- $\text{C}_6\text{F}_2\text{H}_3$), -126.1 (t, $^3J_{\text{FF}} = 14$ Hz, 6F; P(*o*- C_6F_5)₃), -126.6 (m, 3F; P(*p*- C_6F_5)₃), -133.4 (s(br), 8F; B(*o*- C_6F_5)₄), -151.3 (m, 6F; P(*m*- C_6F_5)₃), -164.0 (t, $^3J_{\text{FF}} = 20$ Hz, 4F; B(*p*- C_6F_5)₄), -168.0 ppm (t(br), $^3J_{\text{FF}} = 18$ Hz, 8F; B(*m*- C_6F_5)₄). $^{31}\text{P}\{\text{H}\}$ NMR (202 MHz, CD_2Cl_2): δ = 42.7 ppm (s). $^{13}\text{C}\{\text{H}\}$ NMR (125 MHz, CD_2Cl_2): δ = 107.2 (t, $^3J_{\text{FC}} = 25$ Hz, 1C; 3- $\text{C}_6\text{F}_2\text{H}_3$), 115.2 (d, $^3J_{\text{FC}} = 25$ Hz, 1C; 5- $\text{C}_6\text{F}_2\text{H}_3$), 123.4 (s(br), 1C; 6- $\text{C}_6\text{F}_2\text{H}_3$), 136.2 (d(br), $^1J_{\text{FC}} = 345$ Hz, 8C; B(*o*- C_6F_5)₄), 138.0 (d(br), $^1J_{\text{FC}} = 345$ Hz, 4C; B(*p*- C_6F_5)₄), 139.1 (d(br), $^1J_{\text{FC}} = 380$ Hz, 6C; P(*o*- C_6F_5)₃), 148.0 (d(br), $^1J_{\text{FC}} = 345$ Hz, 8C; B(*m*- C_6F_5)₄), 148.2 (d(br), $^1J_{\text{FC}} = 345$ Hz, 6C; P(*m*- C_6F_5)₃), 149.7 ppm (d(br), $^1J_{\text{FC}} = 345$ Hz, 3C; P(*p*- C_6F_5)₃), resonances for *ipso*-carbons, *p*- $\text{C}_6\text{F}_2\text{H}_3$, and *o*- $\text{C}_6\text{F}_2\text{H}_3$ were not observed. HRMS (TOF-MS EI+): m/z 660.9650 (calcd. for [(2,4- $\text{F}_2\text{PhO})\text{P}(\text{C}_6\text{F}_5)_3]^+: 660.9625); elemental analysis calcd (%) for $\text{C}_{48}\text{H}_3\text{BF}_3\text{OP}$: C, 43.02; H, 0.23; found: C, 42.13; H, 0.25.$

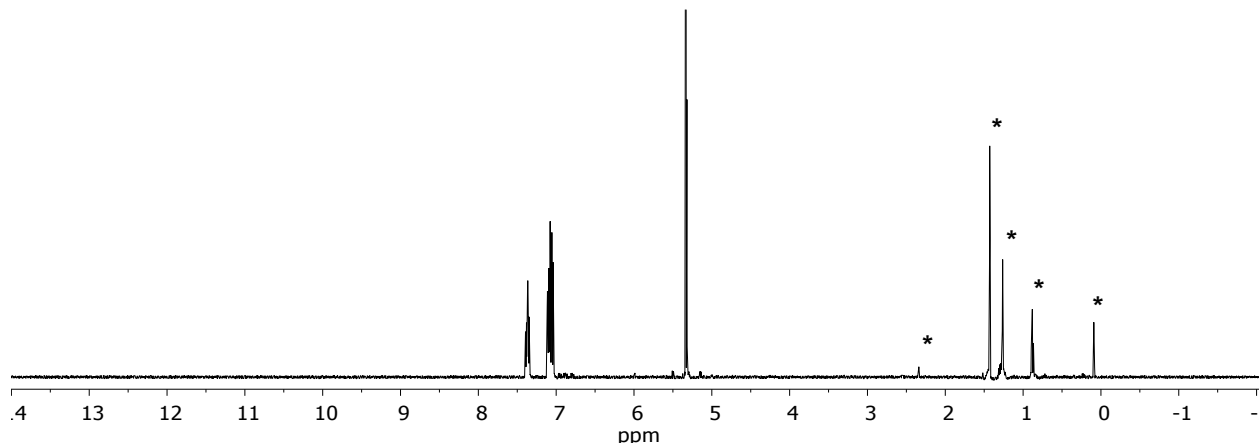


Figure 11. ^1H (CD_2Cl_2) NMR spectrum. Asterisks denote solvent and silicon grease impurities.

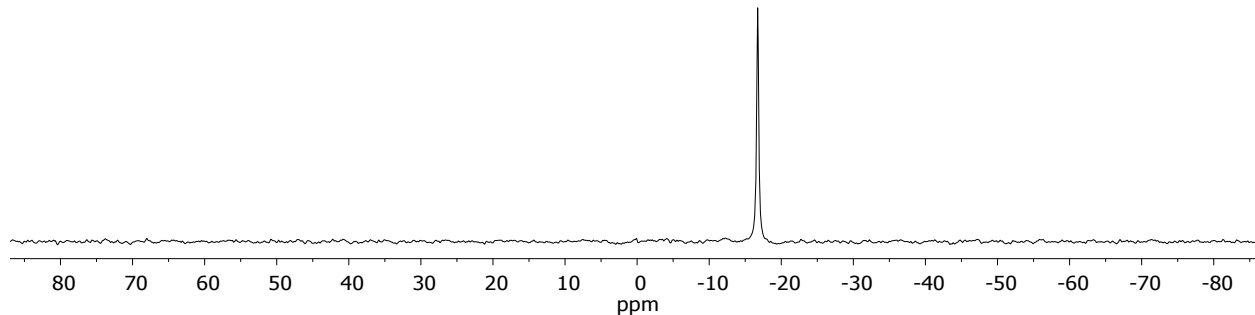


Figure 12. $^{11}\text{B}\{^1\text{H}\}$ (CD_2Cl_2) NMR spectrum.

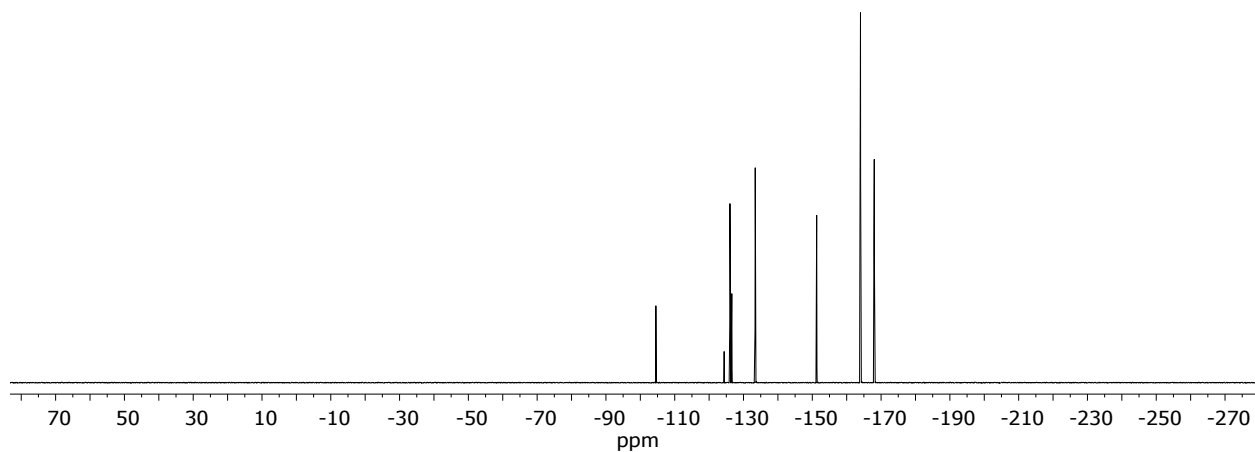


Figure 13. ^{19}F (CD_2Cl_2) NMR spectrum.

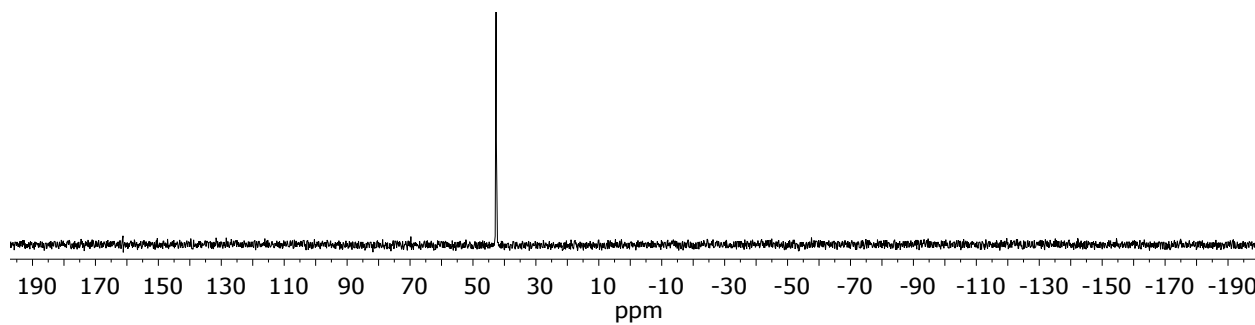


Figure 14. $^{31}\text{P}\{^1\text{H}\}$ (CD_2Cl_2) NMR spectrum.

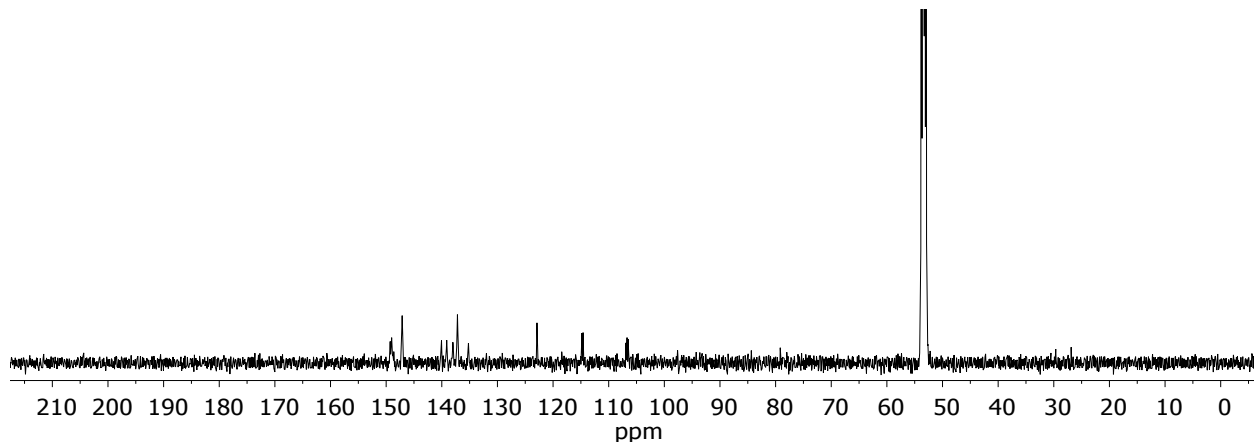


Figure 15. $^{13}\text{C}\{^1\text{H}\}$ (CD_2Cl_2) NMR spectrum.

2.4 $[(\text{C}_6\text{F}_5\text{O})\text{P}(\text{C}_6\text{F}_5)_3][\text{B}(\text{C}_6\text{F}_5)_4]$ (4)

$$\left[\begin{array}{c} \text{OC}_6\text{F}_5 \\ | \\ \text{P} \\ \diagdown \quad \diagup \\ \text{C}_6\text{F}_5 \quad \text{C}_6\text{F}_5 \\ | \\ \text{C}_6\text{F}_5 \end{array} \right]^\oplus \text{ To a solution of } [\text{ClP}(\text{C}_6\text{F}_5)_3][\text{B}(\text{C}_6\text{F}_5)_4] \text{ (580 mg, 0.47 mmol) in } \text{CH}_2\text{Cl}_2 \text{ (20 mL) was added sodium pentafluoro-phenoxide (NaOC}_6\text{F}_5, 144 \text{ mg, 0.7 mmol). The reaction mixture was stirred for 36 h at room temperature, which yielded a white powder and a brown/orange supernatant which was decanted. The powder was washed with a solution of 4 : 6 CH}_2\text{Cl}_2 : n\text{-pentane (3 x 10 mL) and the washing were added to the supernatant, which was then dried in vacuo, washed with n-pentane (3 x 3 mL), and re-dried in vacuo to afford a white powder (506 mg, 78% yield). } ^{11}\text{B}\{^1\text{H}\} \text{ NMR (160 MHz, CD}_2\text{Cl}_2\text{): } \delta = -16.7 \text{ ppm (s). } ^{19}\text{F} \text{ NMR (470 MHz, CD}_2\text{Cl}_2\text{): } \delta = -123.7 \text{ (sept, } ^3J_{\text{FF}} = 10 \text{ Hz, 3F; P}(p\text{-C}_6\text{F}_5)_3\text{), } -125.3 \text{ (t, } ^3J_{\text{FF}} = 14 \text{ Hz, 6F; P}(o\text{-C}_6\text{F}_5)_3\text{), } -133.3 \text{ (s(br), 8F; B}(o\text{-C}_6\text{F}_5)_4\text{), } -148.4 \text{ (t, } ^3J_{\text{FF}} = 22 \text{ Hz, } ^4J_{\text{FF}} = 4 \text{ Hz, 1F; O}(p\text{-C}_6\text{F}_5)\text{, } -149.8 \text{ (m, 6F; P}(m\text{-C}_6\text{F}_5)_3\text{), } -152.6 \text{ (m, 2F; O}(m\text{-C}_6\text{F}_5)\text{, } -155.0 \text{ (m, 2F; O}(o\text{-C}_6\text{F}_5)\text{, } -163.9 \text{ (t, } ^3J_{\text{FF}} = 20 \text{ Hz, 4F; B}(p\text{-C}_6\text{F}_5)_4\text{), } -167.9 \text{ ppm (m(br), 8F; B}(m\text{-C}_6\text{F}_5)_4\text{). } ^{31}\text{P}\{^1\text{H}\} \text{ NMR (202 MHz, CD}_2\text{Cl}_2\text{): } \delta = 47.8 \text{ ppm (s). Poor solubility precluded the acquisition of satisfactory } ^{13}\text{C NMR and } ^{19}\text{F} - ^{13}\text{C HSQC. HRMS (TOF-MS EI+): m/z 714.9340 (calcd. for } [(\text{C}_6\text{F}_5\text{O})\text{P}(\text{C}_6\text{F}_5)_3]^+ : 714.9367); \text{ elemental analysis calcd (\%) for C}_{48}\text{BF}_{40}\text{OP} \bullet \text{CH}_2\text{Cl}_2: \text{C, 39.79; H, 0.147; found: C, 39.39; H, 0.19.}$$

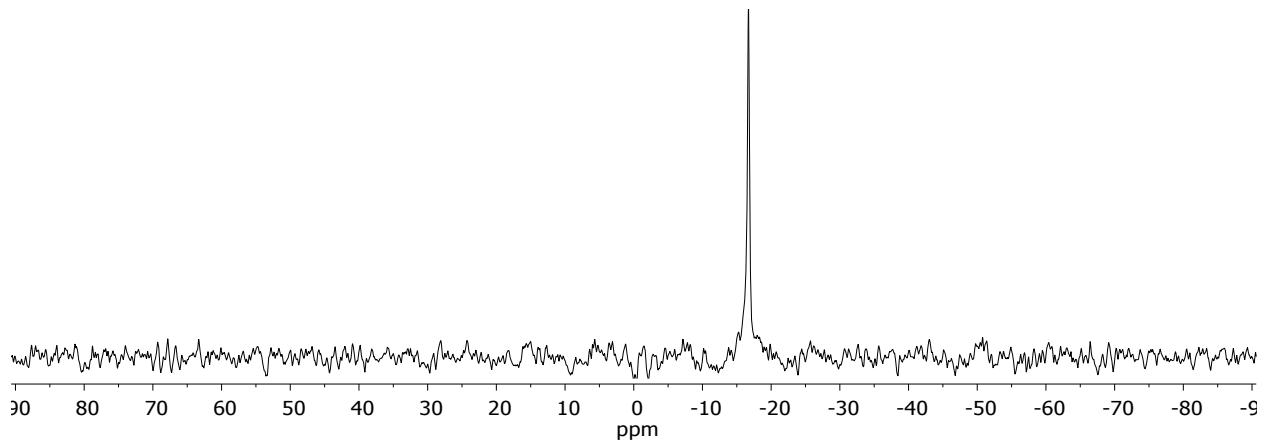


Figure 16. $^{11}\text{B}\{^1\text{H}\}$ (CD_2Cl_2) NMR spectrum.

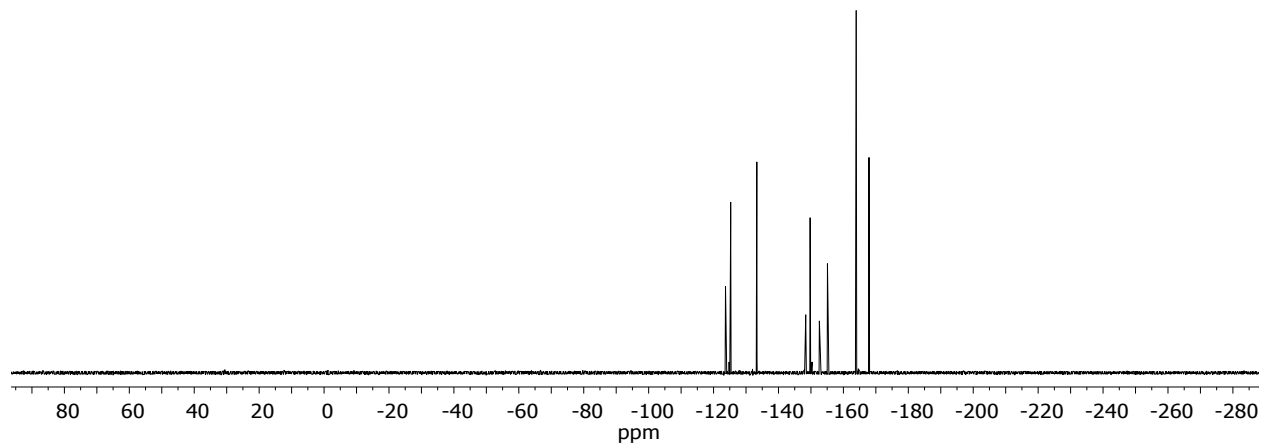


Figure 17. ^{19}F (CD_2Cl_2) NMR spectrum.

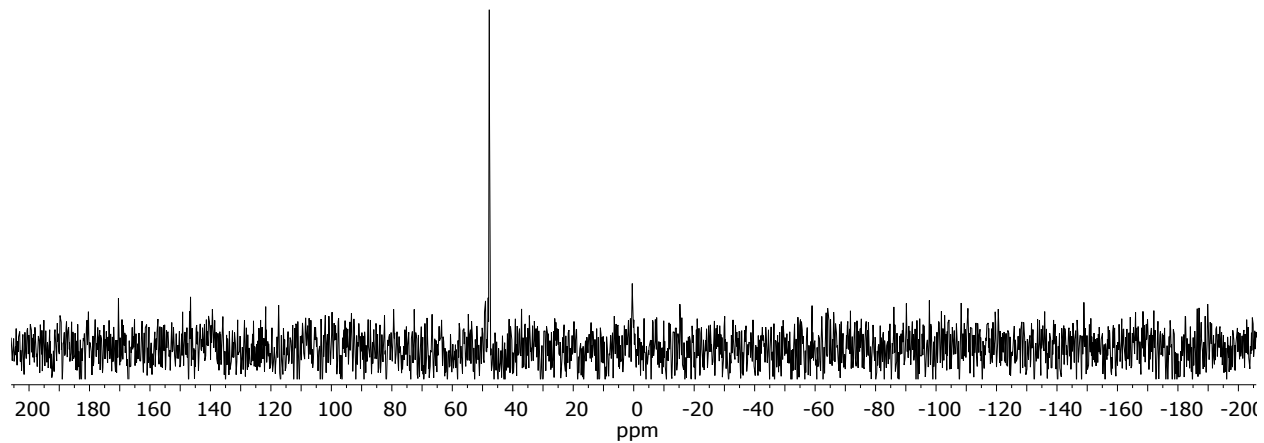
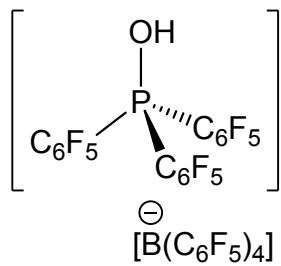


Figure 18. $^{31}\text{P}\{^1\text{H}\}$ (CD_2Cl_2) NMR spectrum.

2.5 $[(HO)P(C_6F_5)_3][B(C_6F_5)_4]$ (5)



To a solution of $[H(OEt_2)_2][B(C_6F_5)_4]$ (15.4 mg, 0.019 mmol) in CH_2Cl_2 (0.6 mL) was added tris(pentafluorophenyl)phosphine oxide ($OP(C_6F_5)_3$, 10 mg, 0.019 mmol). The reaction mixture was left at ambient temperature for 10 min. 1H NMR (500z MHz, CD_2Cl_2): δ = 1.25 (t, $^3J_{CH}$ = 7 Hz, 6H; Et_2O-CH_3), 3.70 (q, $^3J_{CH}$ = 7 Hz, 4H; Et_2O-CH_2), 6.23 ppm (s(br), 1H; P-OH). $^{11}B\{^1H\}$ NMR (128 MHz, CD_2Cl_2): δ = -16.4 ppm (s). ^{19}F NMR (377 MHz, CD_2Cl_2): δ = -131.9 (m(br), 6F; P(*o*-C₆F₅)₃), -133.3 (s(br), 8F; B(*o*-C₆F₅)₄), -140.0 (m, 3F; P(*p*-C₆F₅)₃), -157.3 (m, 6F; P(*m*-C₆F₅)₃), -163.9 (t, $^3J_{FF}$ = 20 Hz, 4F; B(*p*-C₆F₅)₄), -167.7 ppm (t(br), $^1J_{FC}$ = 20 Hz, 8F; B(*m*-C₆F₅)₄). $^{31}P\{^1H\}$ NMR (162 MHz, CD_2Cl_2): δ = -3.2 ppm (s(br)). $^{13}C\{^1H\}$ NMR (125 MHz, CD_2Cl_2): δ = 14.5 (s, 2C; Et_2O-CH_3), 67.6 (s, 2C; Et_2O-CH_2), 136.2 (d(br), $^1J_{FC}$ = 240 Hz, 8C; B(*o*-C₆F₅)₄), 138.2 (d(br), $^1J_{FC}$ = 240 Hz, 4C; B(*p*-C₆F₅)₄), 147.0 (d(br), $^1J_{FC}$ = 260 Hz, 6C; P(*o*-C₆F₅)₃), 148.1 (d(br), $^1J_{FC}$ = 240 Hz, 8C; B(*m*-C₆F₅)₄), 146.0 (d(br), $^1J_{FC}$ = 260 Hz, 6C; P(*p*-C₆F₅)₃), 138.3 ppm (d(br), $^1J_{FC}$ = 260 Hz, 3C; P(*p*-C₆F₅)₃), resonance for *ipso*-carbons was not observed. HRMS (ESI+): m/z 548.95160 (calcd. for $[(HO)P(C_6F_5)_3]^+$: 548.95255).

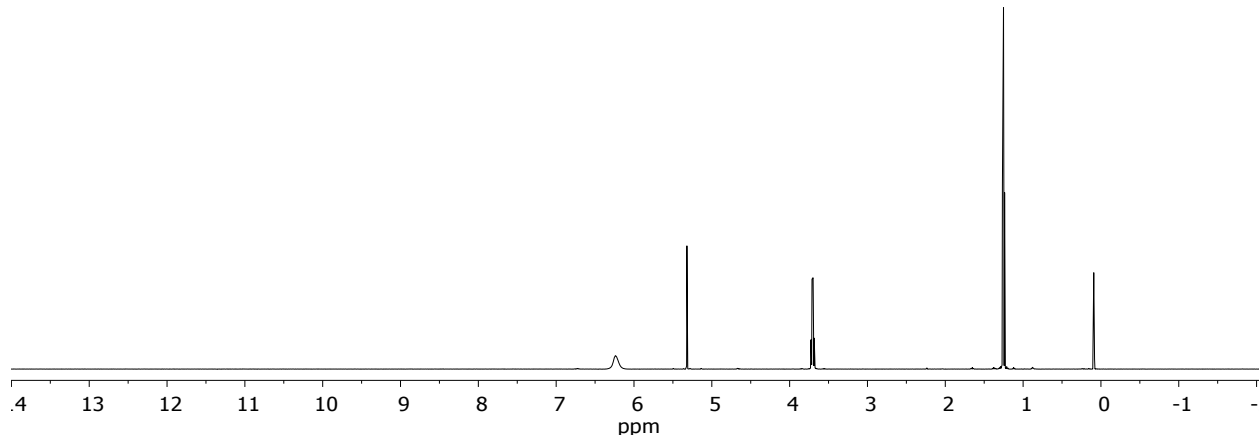


Figure 19. 1H (CH_2Cl_2) NMR spectrum.

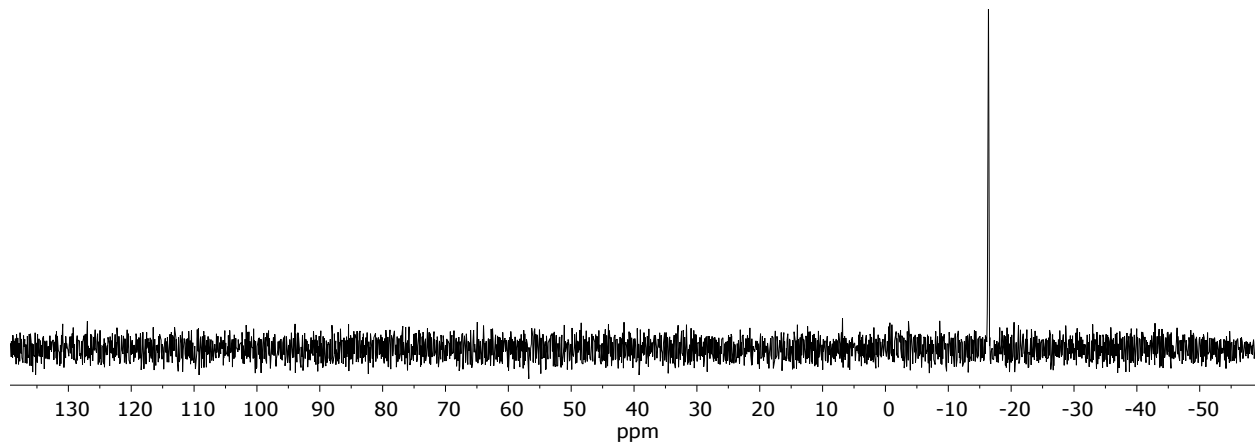


Figure 20. $^{11}\text{B}\{^1\text{H}\}$ (CH_2Cl_2) NMR spectrum.

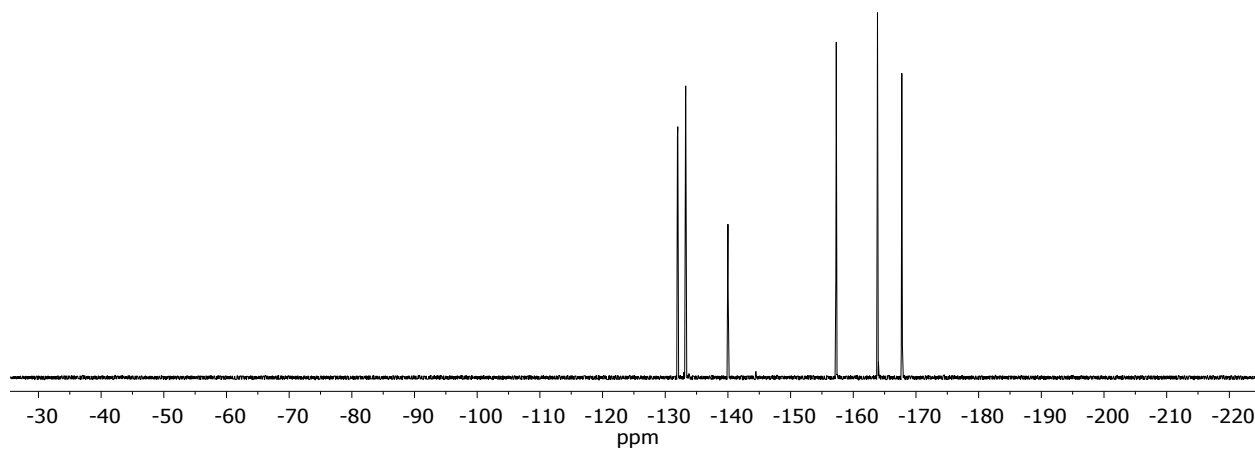


Figure 21. ^{19}F (CH_2Cl_2) NMR spectrum.

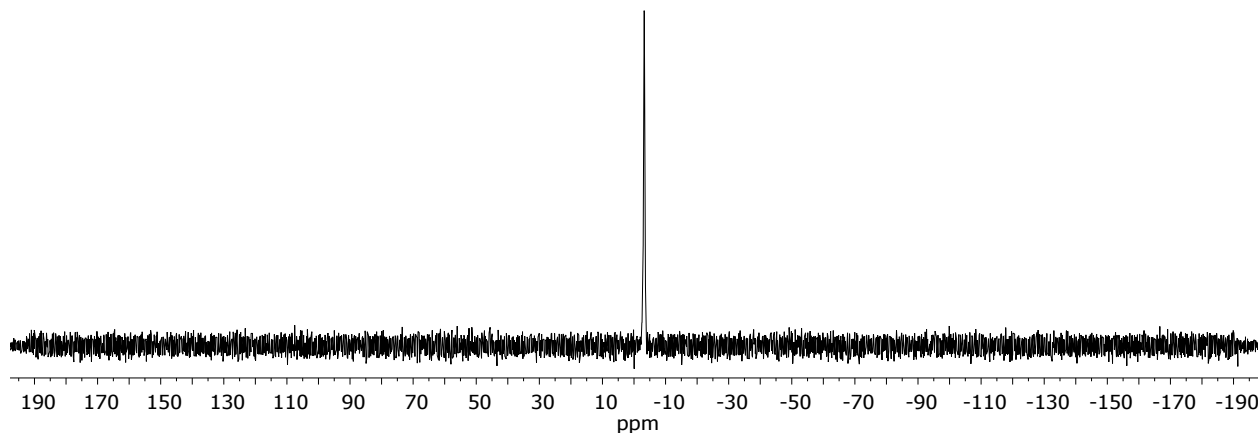


Figure 22. $^{31}\text{P}\{^1\text{H}\}$ (CH_2Cl_2) NMR spectrum.

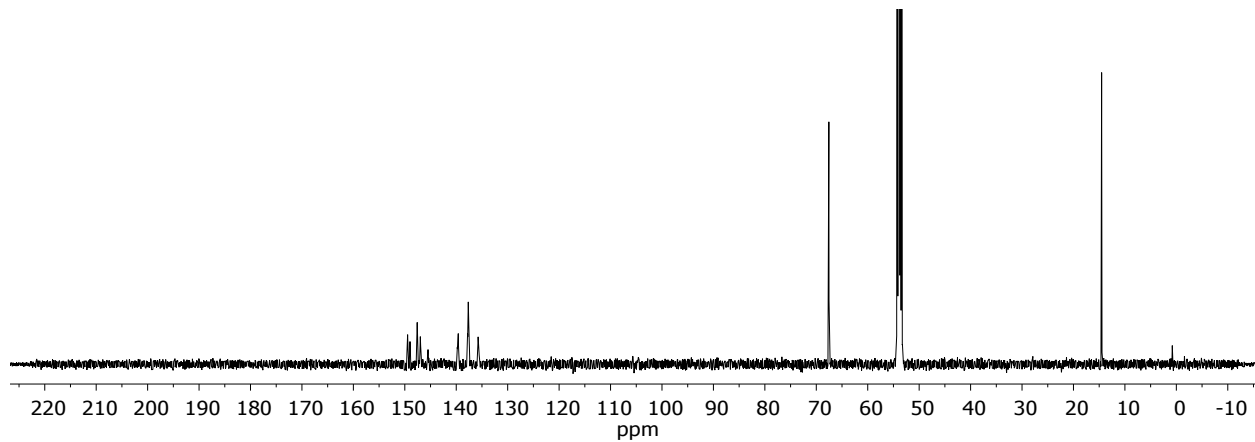
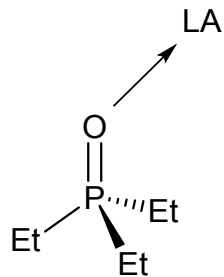


Figure 23. $^{13}\text{C}\{^1\text{H}\}$ (CH_2Cl_2) NMR spectrum.

3. Gutmann-Beckett Test



In a 20 mL vial, a solution of the phosphonium catalyst (0.02 mmol) was prepared in 0.6 mL CH_2Cl_2 and added to a separate vial containing Et_3PO (0.02 mmol). The solution was transferred to an NMR tube and monitored by ^{31}P and ^{19}F NMR spectroscopy after 1 h at ambient temperature (unless otherwise specified).

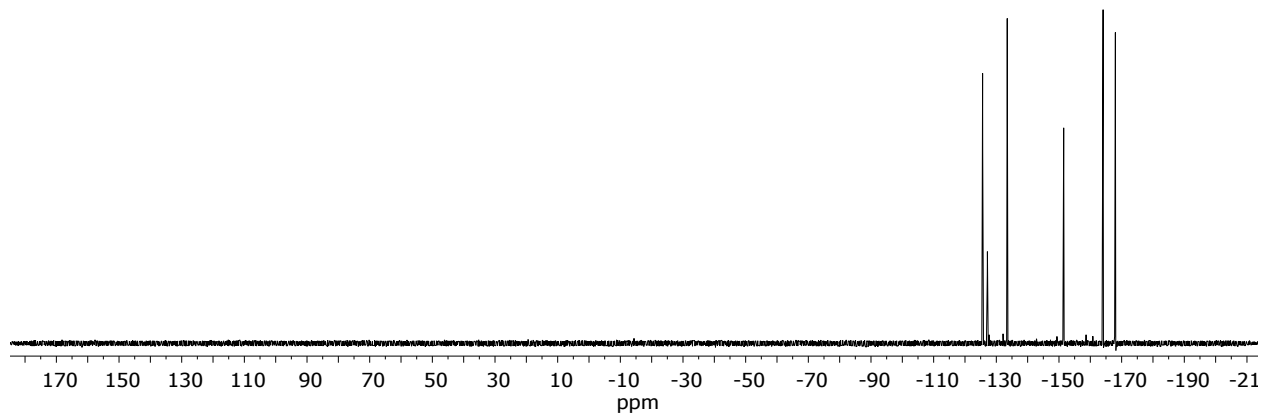


Figure 24. ^{19}F (CH_2Cl_2) NMR spectrum of Gutmann-Beckett test with **1**.

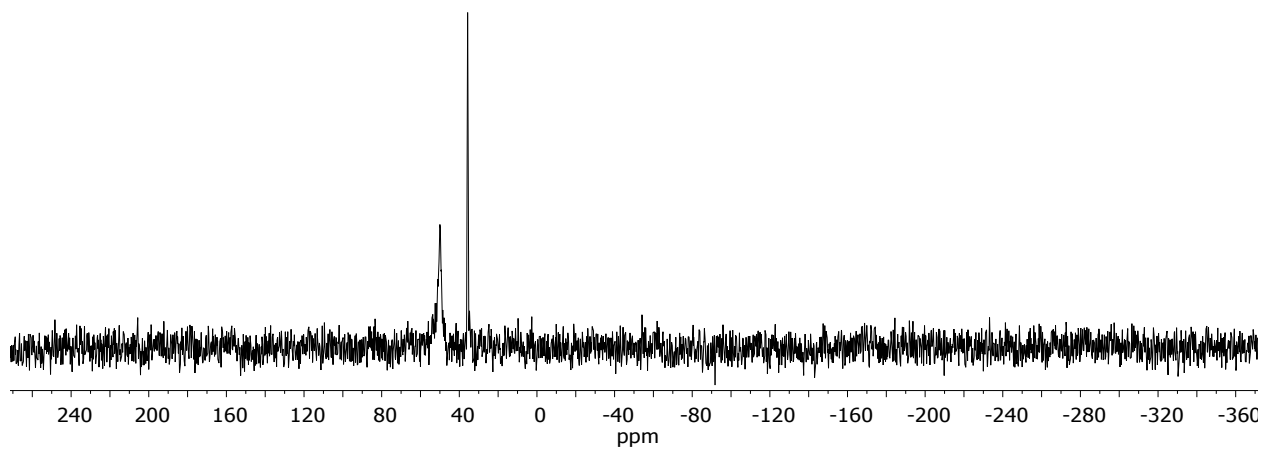


Figure 25. $^{31}\text{P}\{^1\text{H}\}$ (CH_2Cl_2) NMR spectrum of Gutmann-Beckett test with **1**.

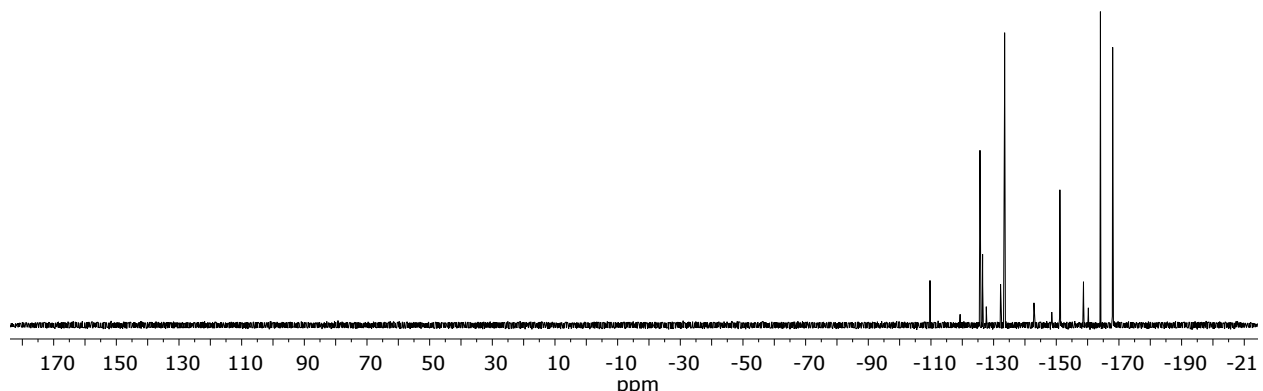


Figure 26. ^{19}F (CH_2Cl_2) NMR spectrum of Gutmann-Beckett test with **2**.

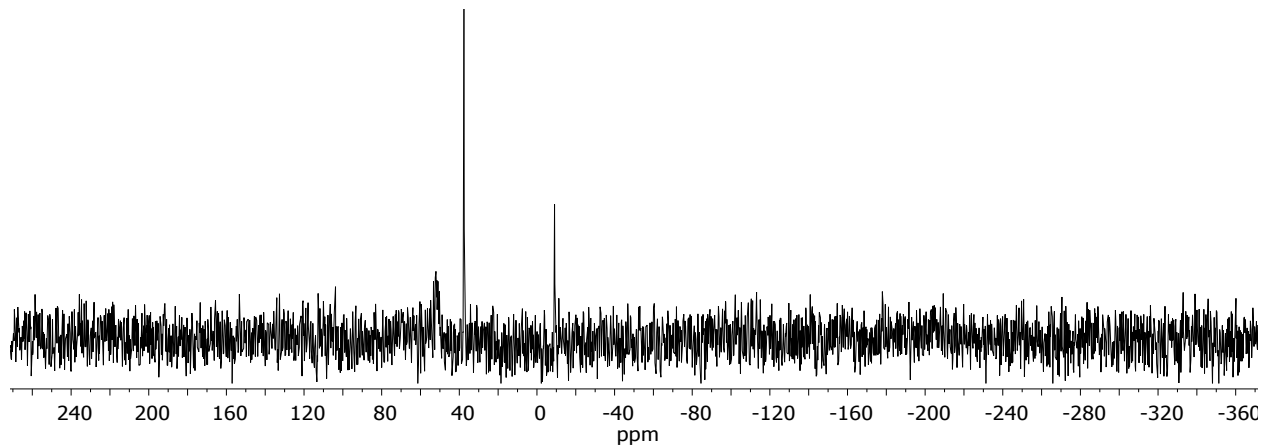


Figure 27. $^{31}\text{P}\{\text{H}\}$ (CH_2Cl_2) NMR spectrum of Gutmann-Beckett test with **2**.

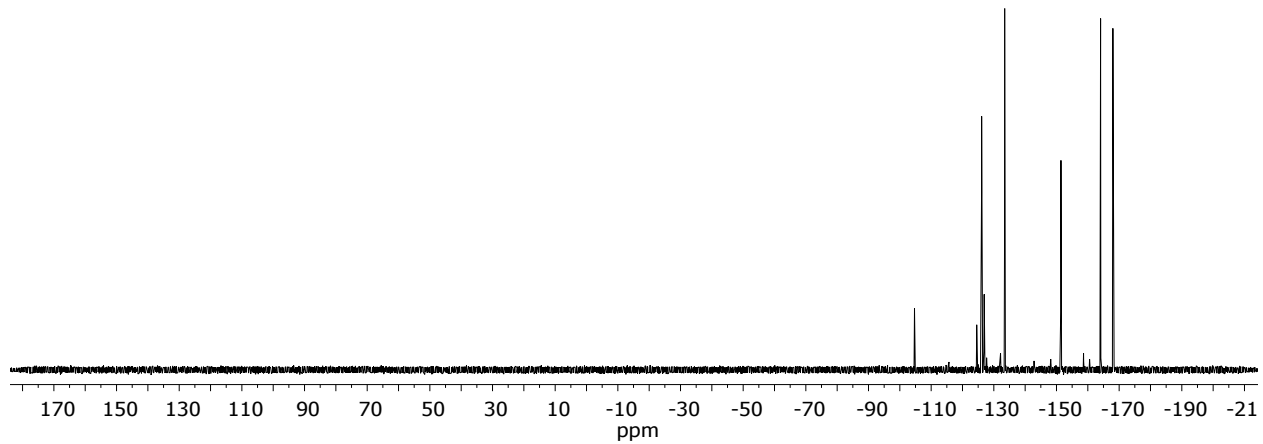


Figure 28. ^{19}F (CH_2Cl_2) NMR spectrum of Gutmann-Beckett test with **3**.

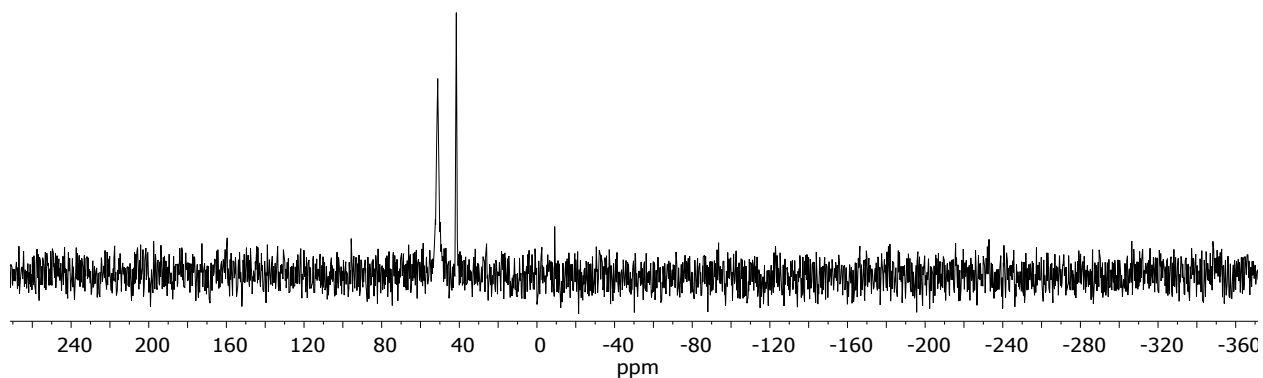


Figure 29. $^{31}\text{P}\{\text{H}\}$ (CH_2Cl_2) NMR spectrum of Gutmann-Beckett test with **3**.

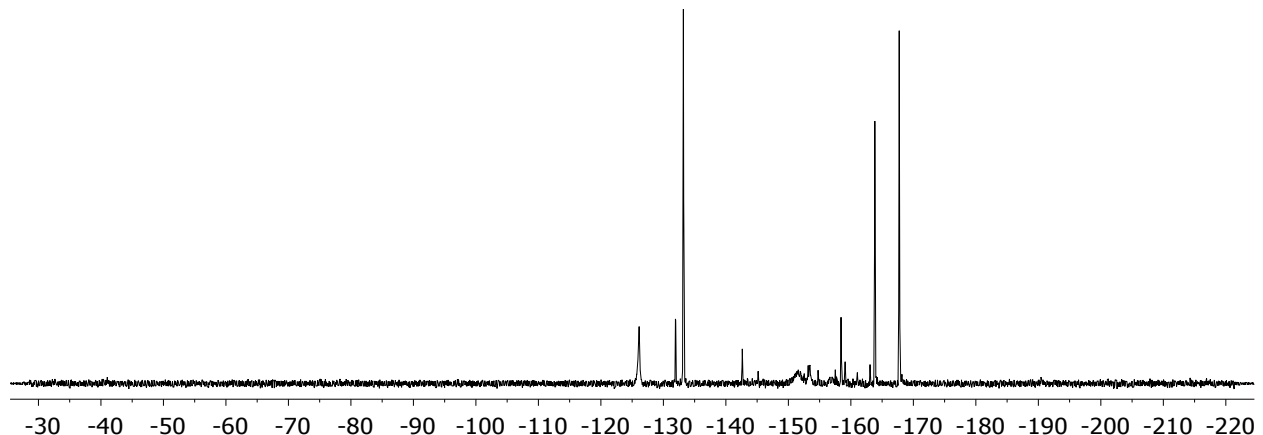


Figure 30. ^{19}F (CH_2Cl_2) NMR spectrum of Gutmann-Beckett test with **4**.

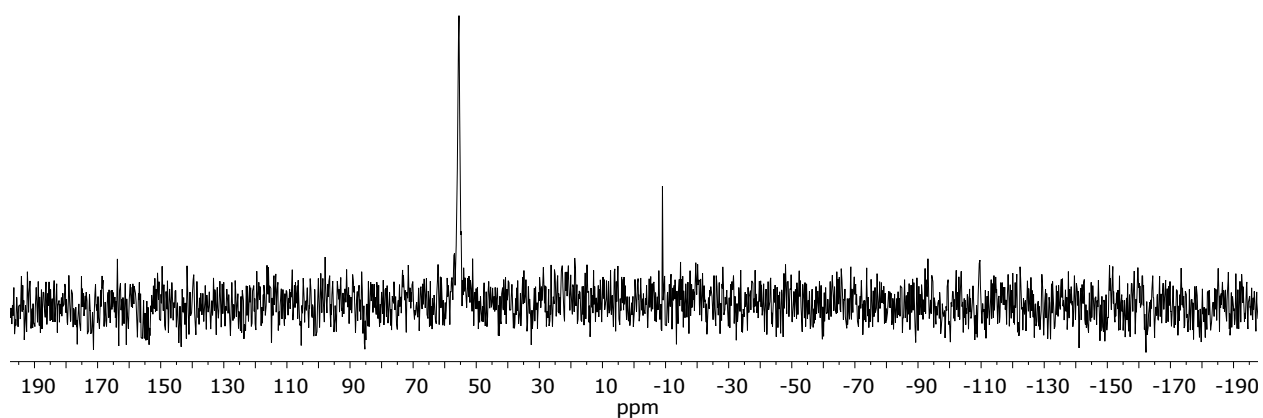
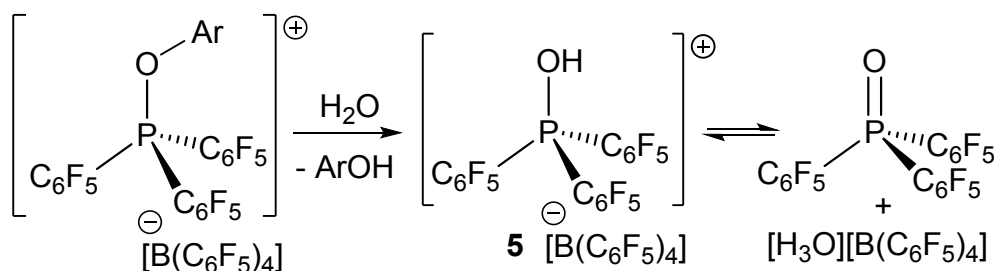


Figure 31. $^{31}\text{P}\{^1\text{H}\}$ (CH_2Cl_2) NMR spectrum of Gutmann-Beckett test with **4**.

4. Air Stability Test

4.1 Air Stability of Cations 1-4



In a 20 mL vial, a solution of the phosphonium catalyst (0.02 mmol) was prepared in 0.6 mL CH_2Cl_2 . The solution was transferred to an NMR tube and exposed to atmospheric moisture for specific amounts of time. The decomposition was monitored by ^{19}F NMR spectroscopy.

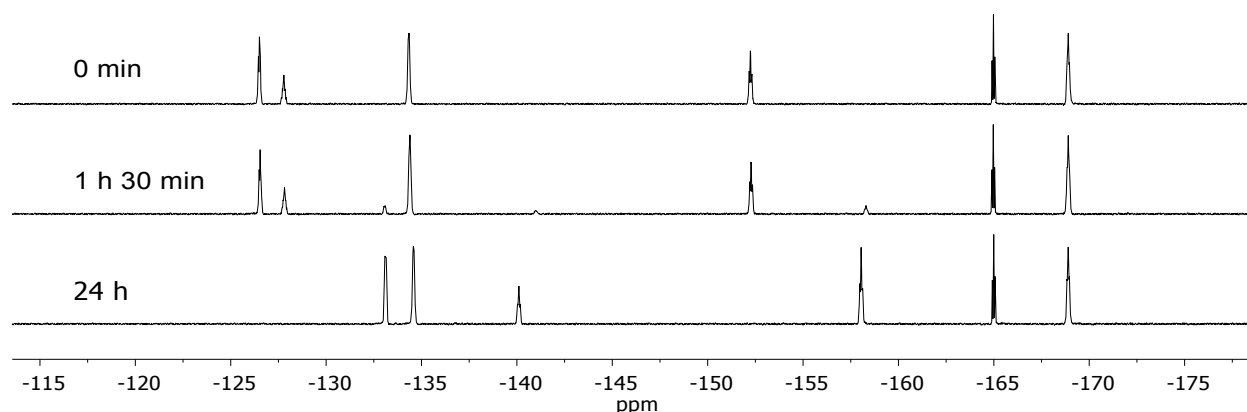


Figure 32. ^{19}F (CH_2Cl_2) NMR spectrum of **1** after exposure to air.

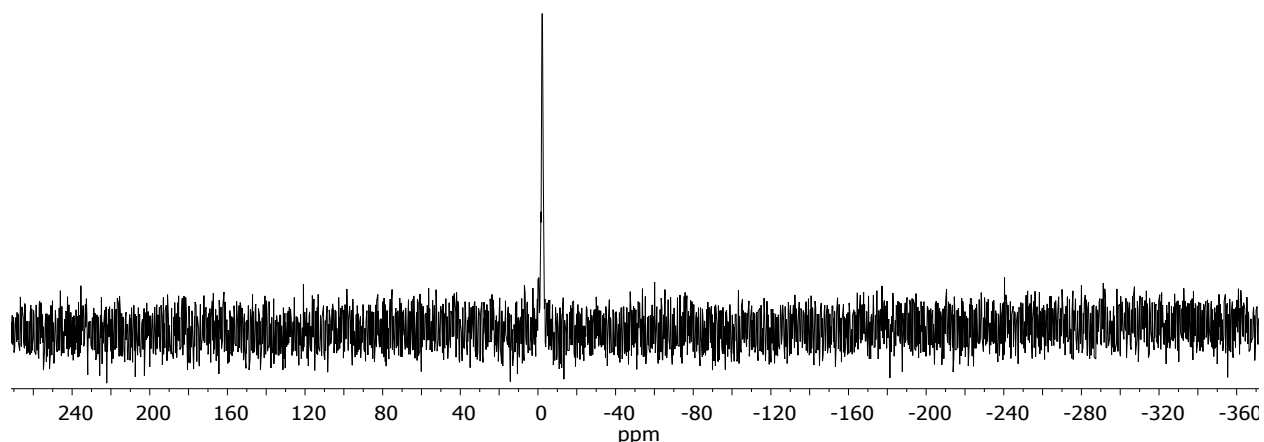


Figure 33. $^{31}P\{^1H\}$ (CH_2Cl_2) NMR spectrum of **1** after exposure to air for 24 h.

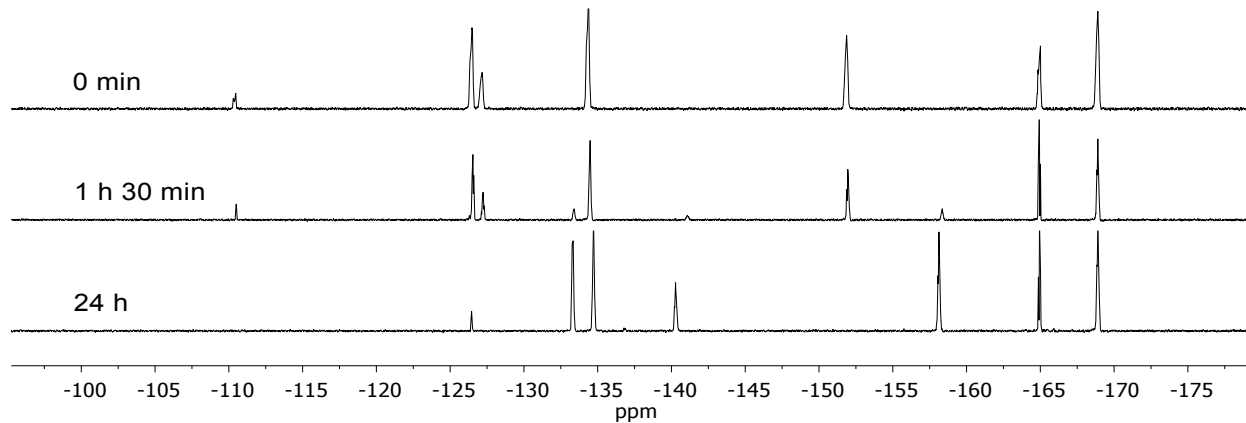


Figure 34. ^{19}F (CH_2Cl_2) NMR spectrum of **2** after exposure to air.

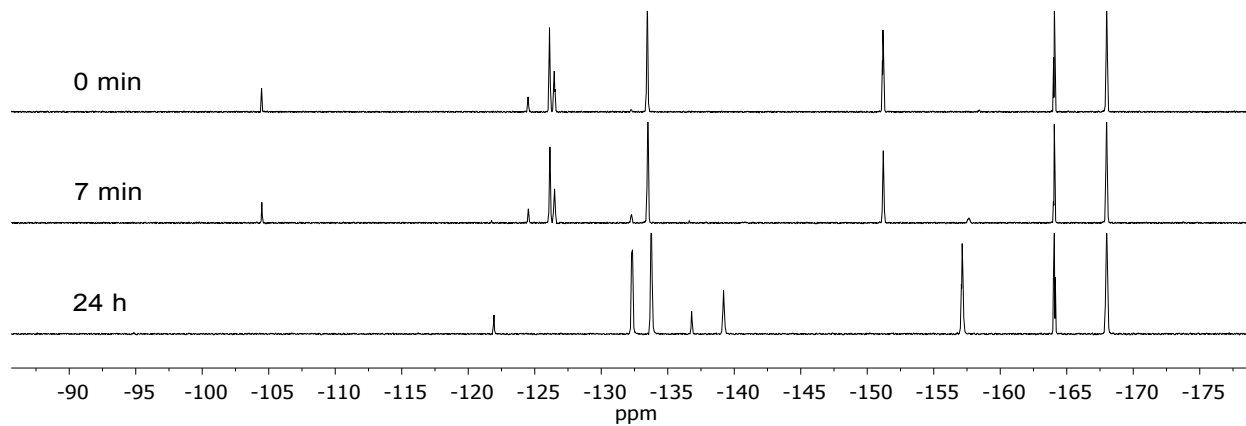


Figure 35. ^{19}F (CH_2Cl_2) NMR spectrum of **3** after exposure to air.

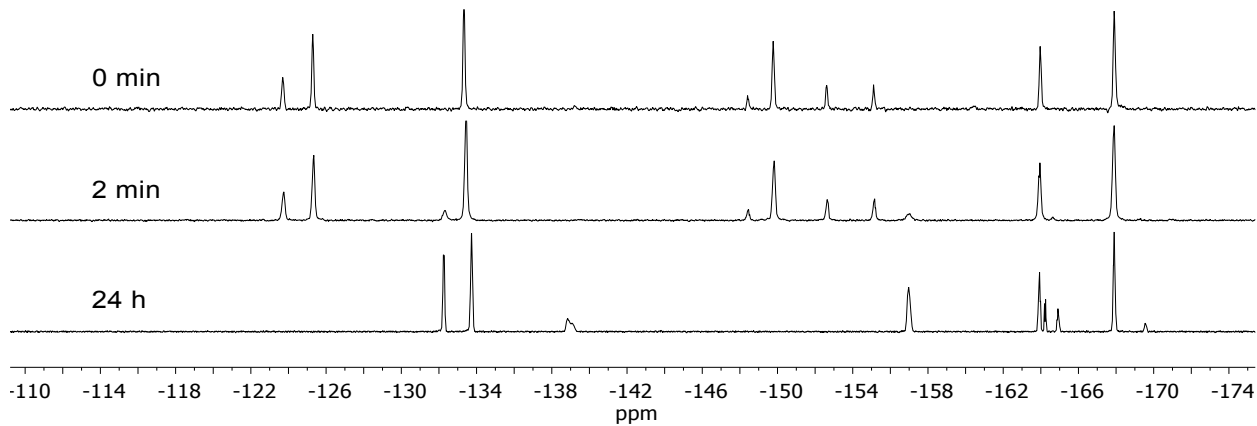


Figure 36. ^{19}F (CH_2Cl_2) NMR spectrum of **4** after exposure to air.

4.2 Identification of Decomposition Product of 1-4

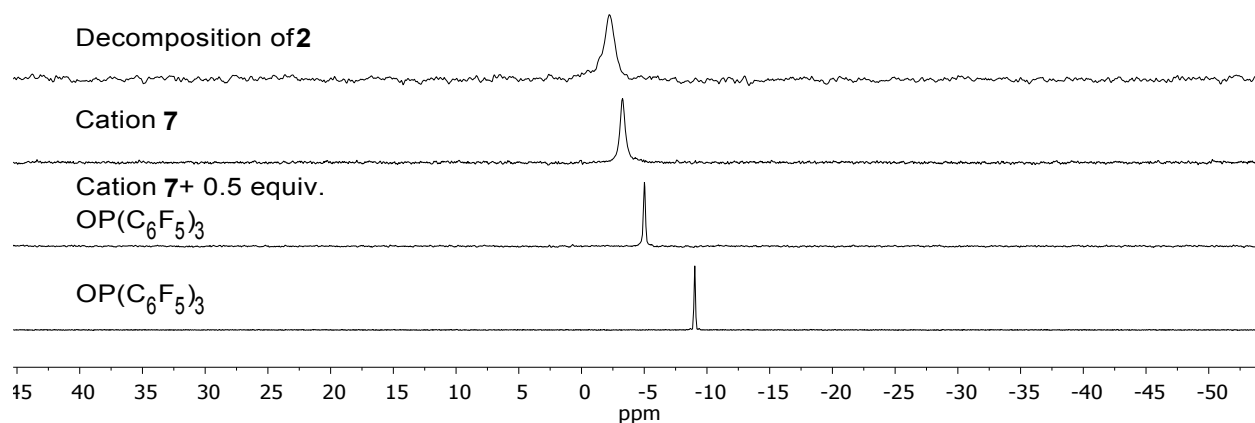


Figure 37. $^{31}\text{P}\{\text{H}\}$ (CH_2Cl_2) NMR spectrum for identification of decomposition product 1-4.

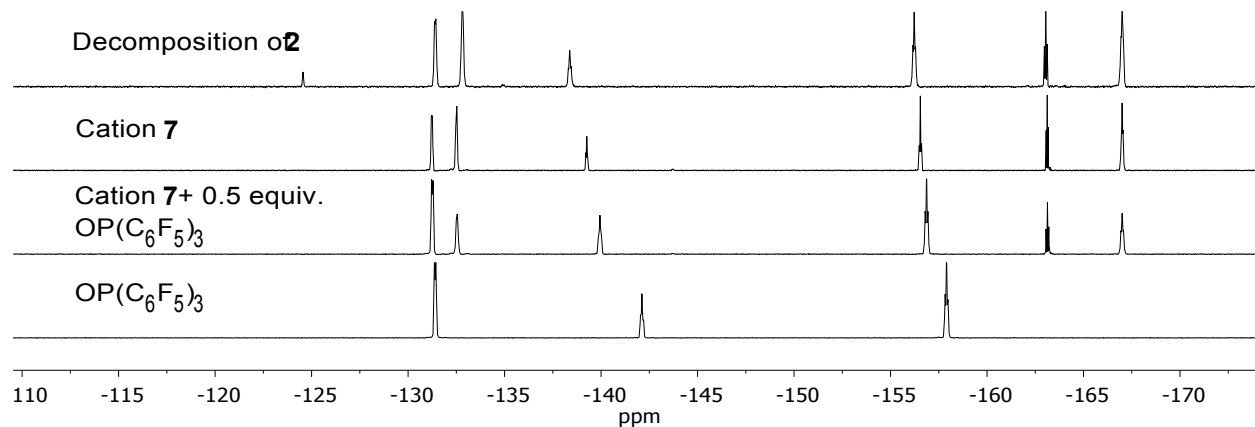


Figure 38. ^{19}F (CH_2Cl_2) NMR spectrum for identification of decomposition product of 1-4.

4.3 Air Stability of $[FP(C_6F_5)_3][B(C_6F_5)_4]$ and Decomposition Product Identification

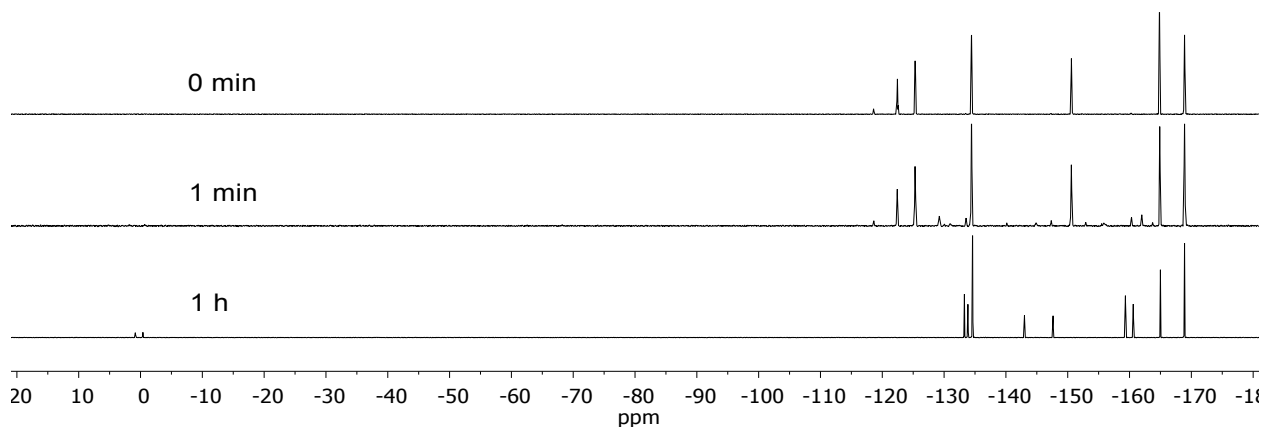


Figure 39. ^{19}F (CH_2Cl_2) NMR spectrum of $[FP(C_6F_5)_3][B(C_6F_5)_4]$ after exposure to air.

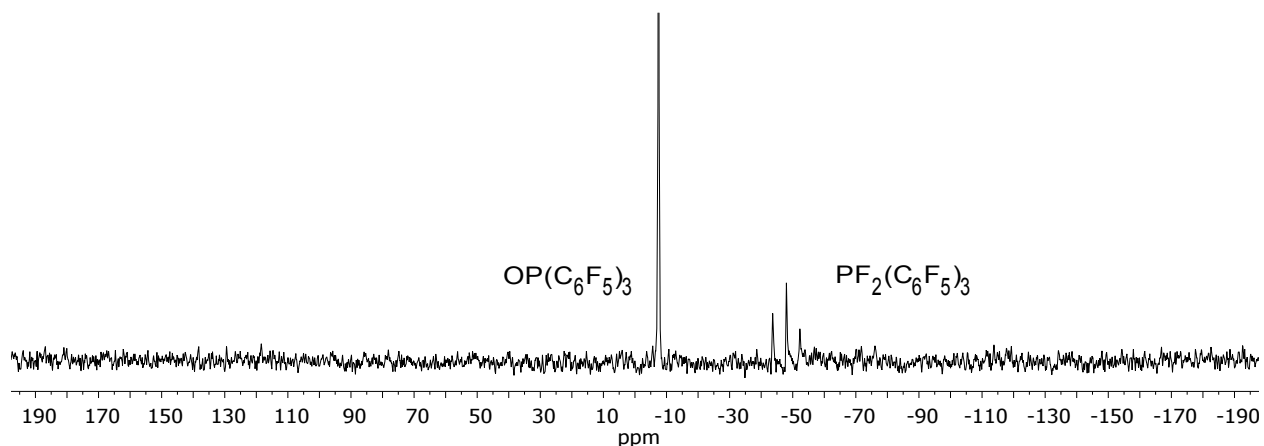


Figure 40. $^{31}\text{P}\{\text{H}\}$ (CH_2Cl_2) NMR spectrum of $[FP(C_6F_5)_3][B(C_6F_5)_4]$ after exposure to air for 1 h.

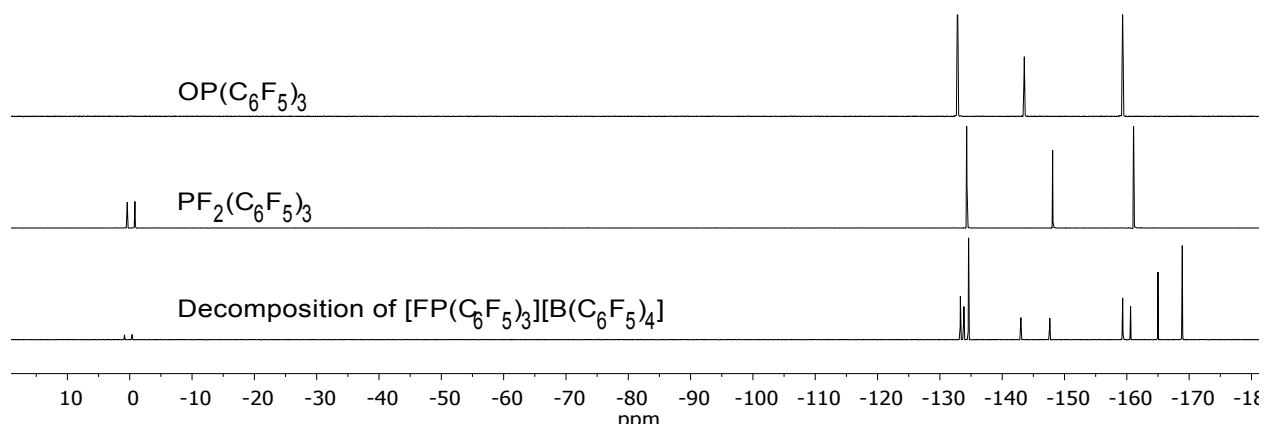
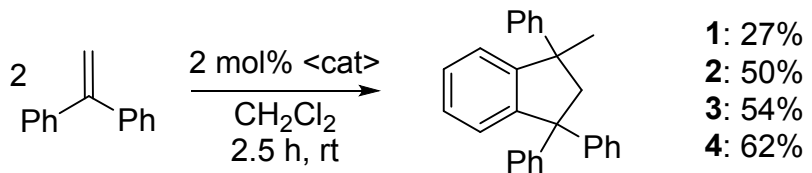


Figure 41. ^{19}F (CH_2Cl_2) NMR spectrum for identification of decomposition product of $[FP(C_6F_5)_3][B(C_6F_5)_4]$.

5. Lewis Acid Catalysis

5.1 Dimerization of 1,1-diphenylethylene



In a 20 mL vial, a solution of the phosphonium catalyst (2 mol%) was prepared in 1 mL CH_2Cl_2 . 1,1-diphenylethylene (0.2 mmol) was added at ambient temperature and the reaction mixture was left to stir for 2.5 h. The solution was then dried *in vacuo* and re-dissolved in 0.6 mL CDCl_3 affording a pale green solution. Conversions were determined by ^1H NMR spectroscopy. Mesitylene was added as an internal standard. Product ^1H NMR spectra are consistent with reference spectra.^[7]

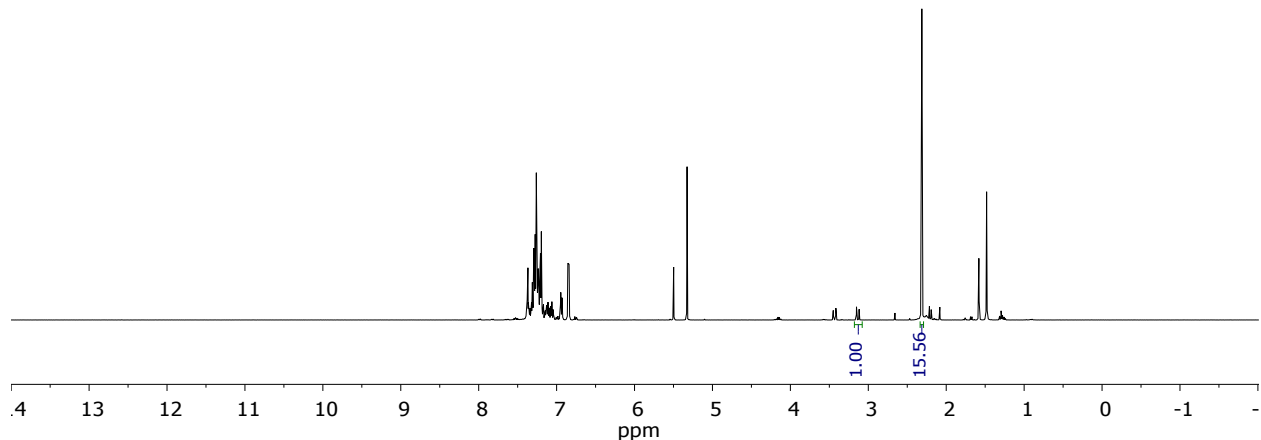


Figure 42. ^1H (CDCl_3) NMR spectrum of catalysis with **1** with mesitylene internal standard (4.1 equiv.).

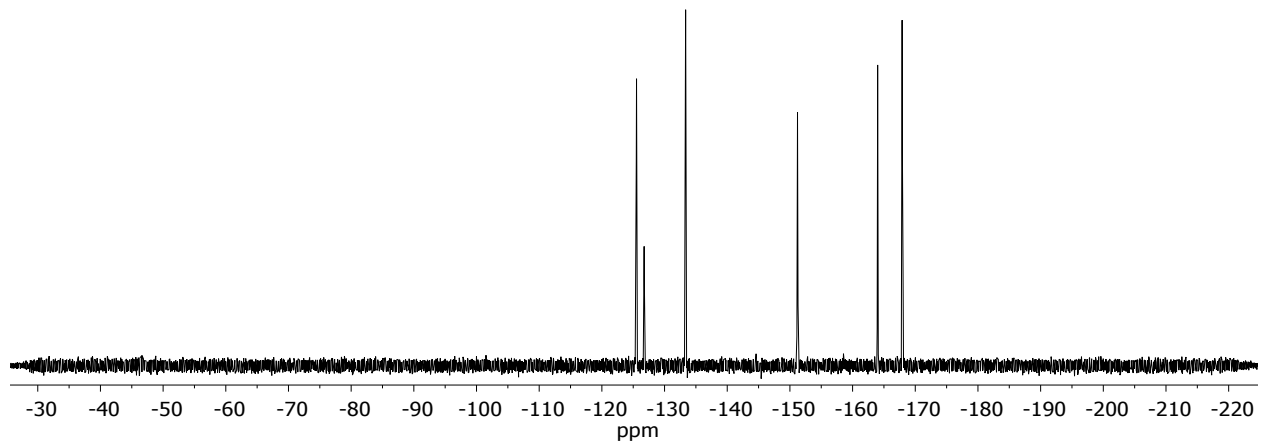


Figure 43. ^{19}F (CH_2Cl_2) NMR spectrum of **1** after catalysis.

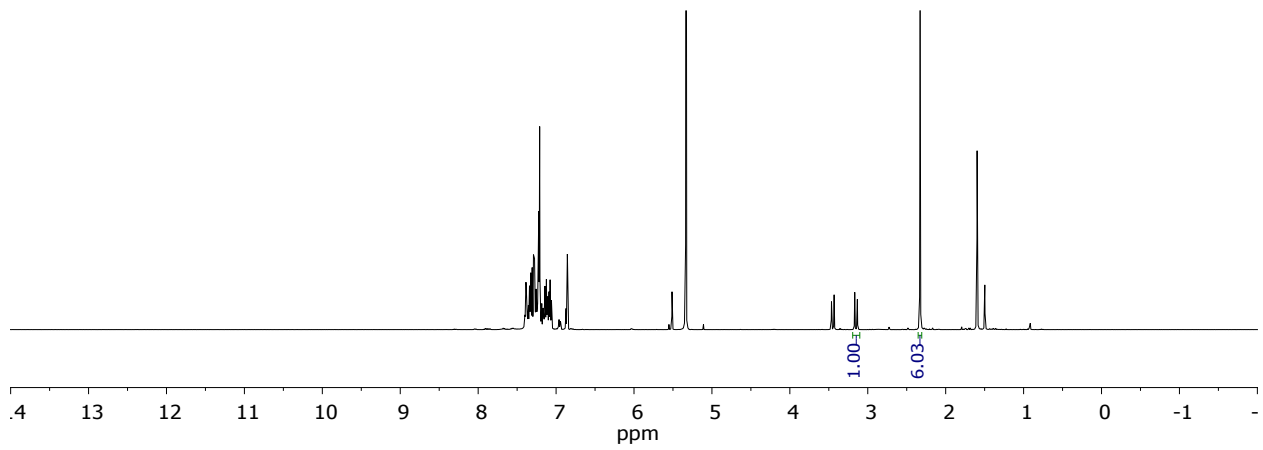


Figure 44. ^1H (CDCl_3) NMR spectrum of catalysis with **2** with mesitylene internal standard (5.3 equiv.).

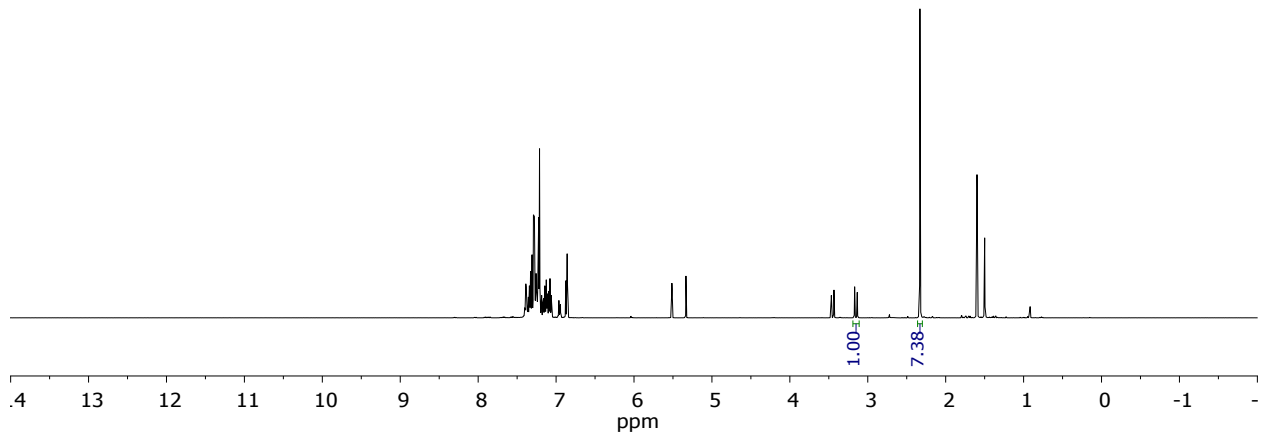


Figure 45. ^1H (CDCl_3) NMR spectrum of catalysis with **3** with mesitylene internal standard (4.6 equiv.).

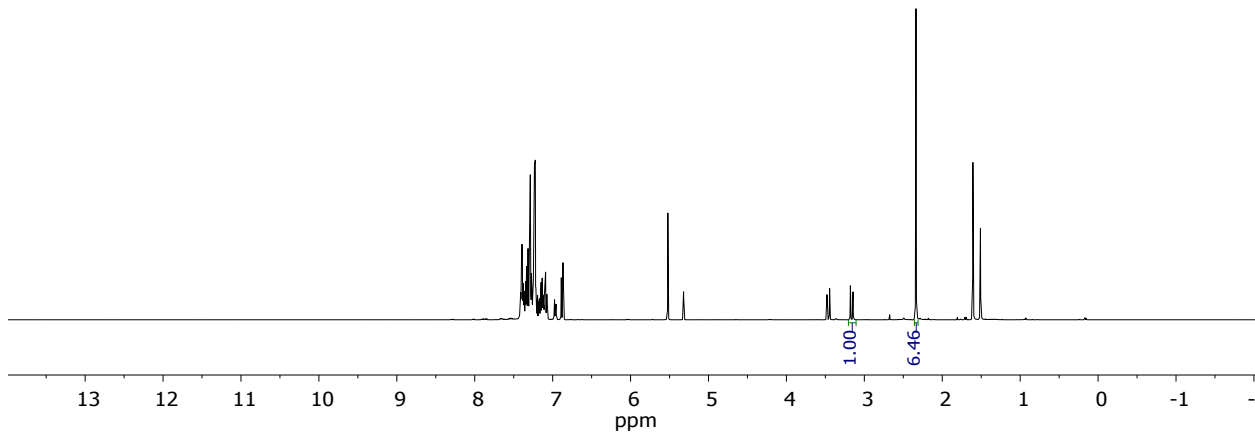


Figure 46. ¹H (CDCl₃) NMR spectrum of catalysis with **4** with mesitylene internal standard (4.3 equiv.).

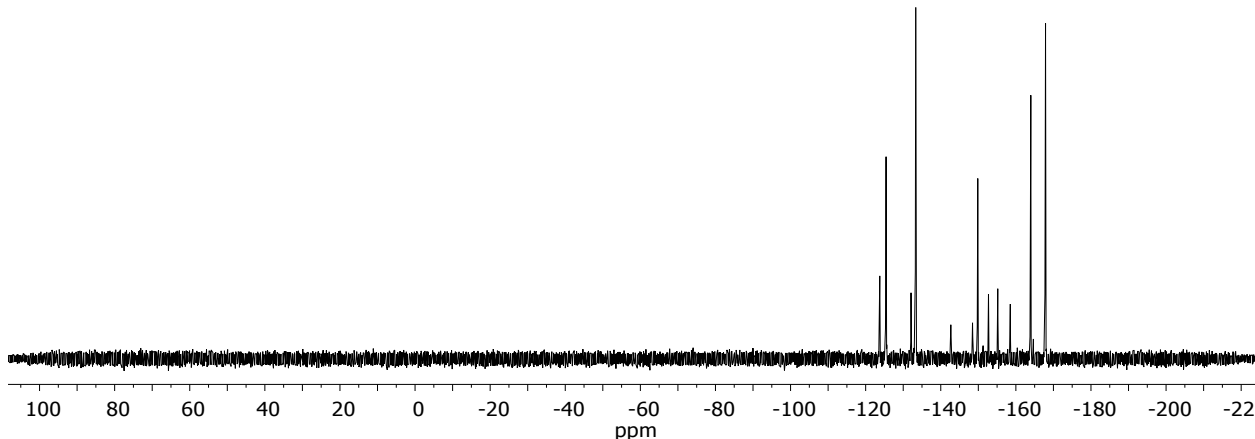
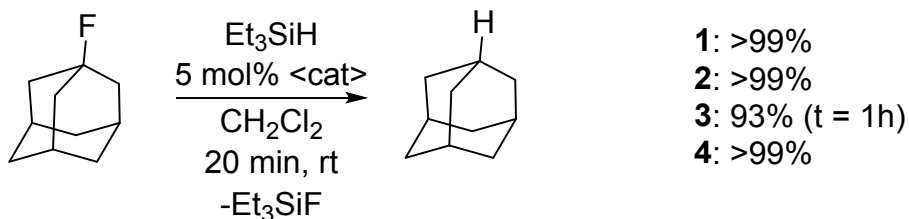


Figure 47. ¹⁹F (CH₂Cl₂) NMR spectrum of **4** after catalysis. Some OP(C₆F₅)₃ is observed.

5.2 Hydrodefluorination of 1-fluoroadamantane



In a 20 mL vial, a solution of the phosphonium catalyst (5 mol%) was prepared in 0.6 mL CH₂Cl₂. Triethylsilane (Et₃SiH, 0.04 mmol) was added at ambient temperature, the reaction was briefly stirred, and then 1-fluoroadamantane was added (0.04 mmol). The reaction mixture was transferred to an NMR tube and left at ambient temperature for 30 min or 1 h, before being

monitored by ^{19}F NMR spectroscopy. Conversions were determined from the proportion of Si-F bonds formed relative to a fluorobenzene internal standard. Product ^1H NMR spectra are consistent with reference spectra.^[8]

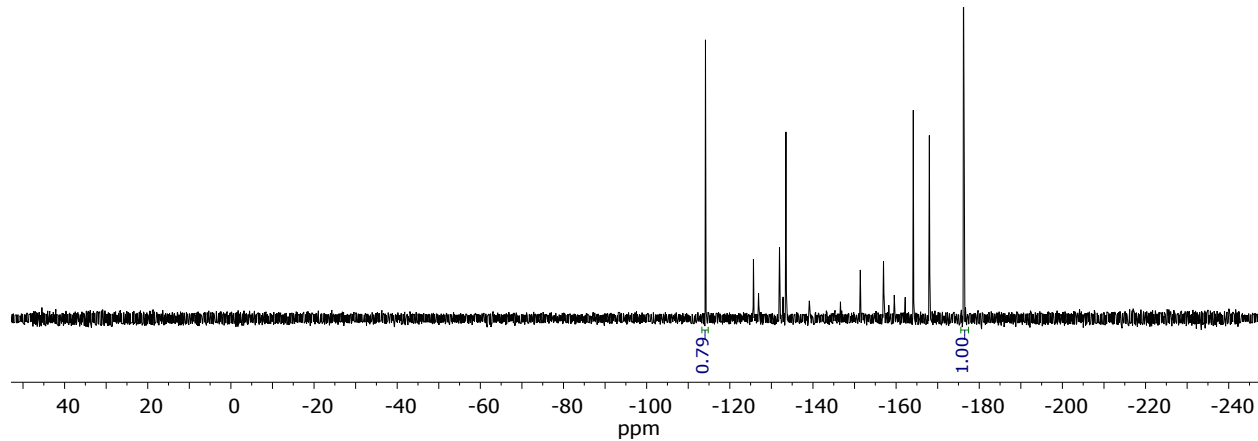


Figure 48. $^{19}\text{F}\{^1\text{H}\}$ (CH_2Cl_2) NMR spectrum of catalysis with **1** with fluorobenzene internal standard (3.4 equiv.). Some decomposition to $\text{PF}_2(\text{C}_6\text{F}_5)_3$ and $\text{OP}(\text{C}_6\text{F}_5)_3$ observed.

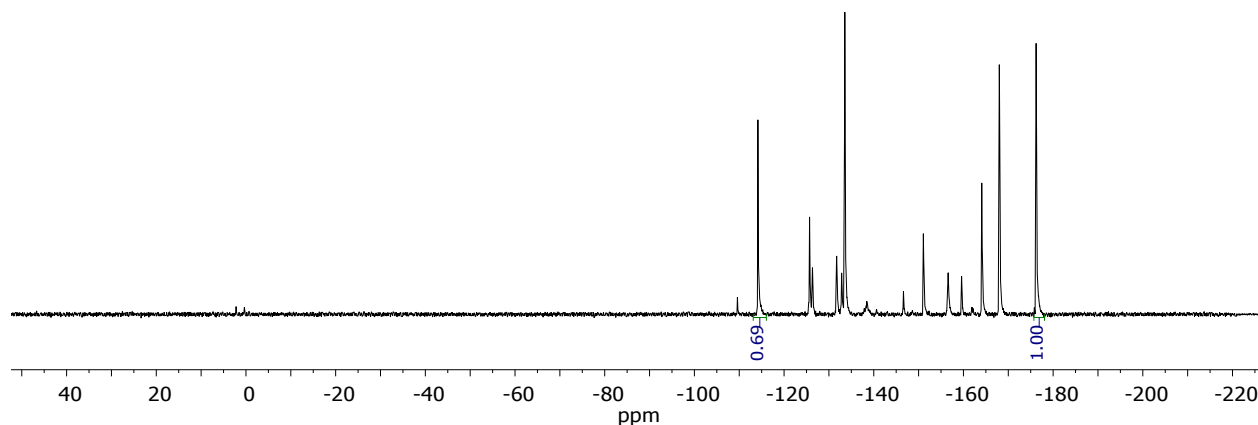


Figure 49. $^{19}\text{F}\{^1\text{H}\}$ (CH_2Cl_2) NMR spectrum of catalysis with **2** with fluorobenzene internal standard (4.1 equiv.). Some formation of $\text{PF}_2(\text{C}_6\text{F}_5)_3$ and $\text{OP}(\text{C}_6\text{F}_5)_3$ is observed.

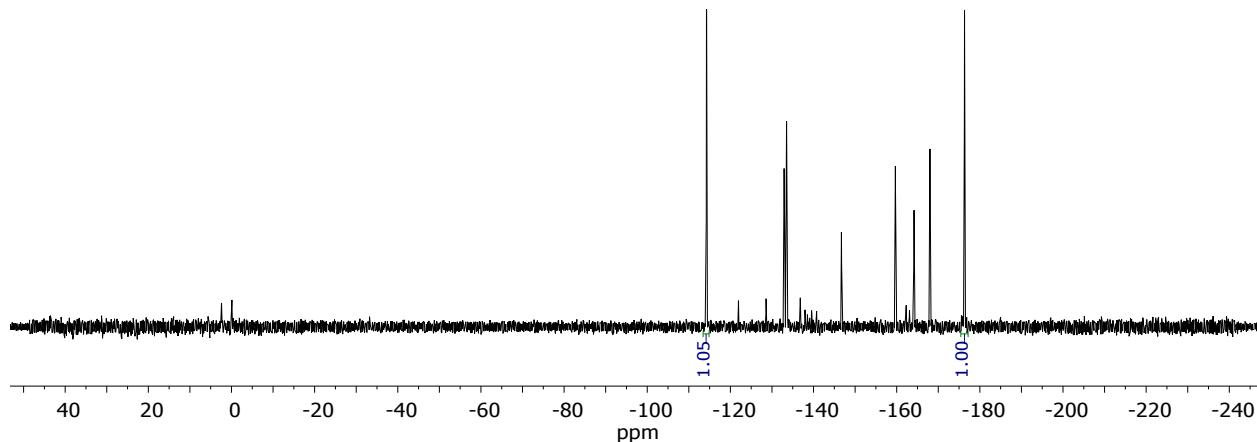


Figure 50. $^{19}\text{F}\{^1\text{H}\}$ (CH_2Cl_2) NMR spectrum of catalysis with **3** with fluorobenzene internal standard (1.0 equiv.). Some formation of $\text{PF}_2(\text{C}_6\text{F}_5)_3$ and $\text{OP}(\text{C}_6\text{F}_5)_3$ is observed.

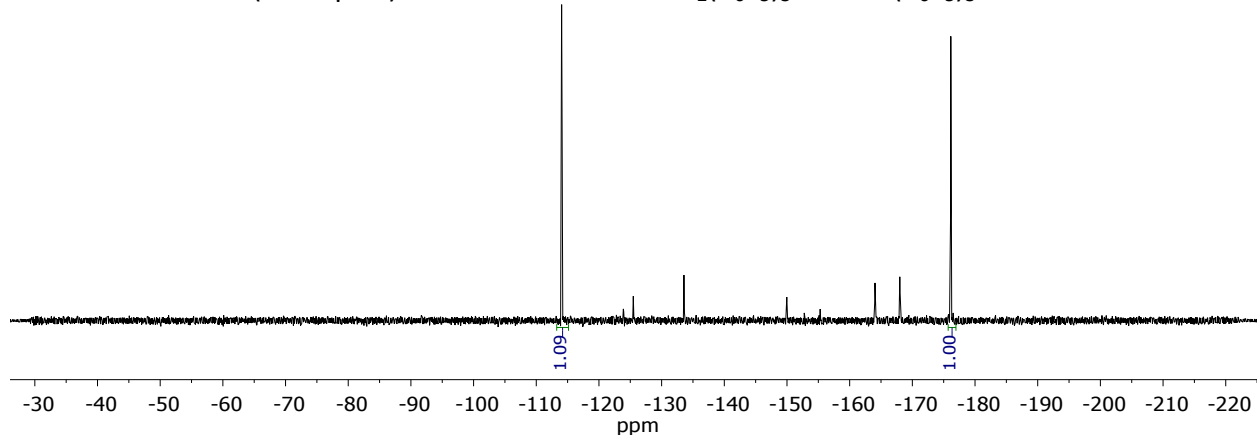
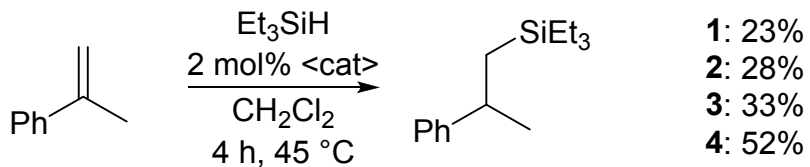


Figure 51. $^{19}\text{F}\{^1\text{H}\}$ (CH_2Cl_2) NMR spectrum of catalysis with **4** with fluorobenzene internal standard (7.8 equiv.).

5.3 Hydrosilylation of α -methylstyrene



In a 20 mL vial, a solution of the phosphonium catalyst (2 mol%) was prepared in 0.6 mL CH_2Cl_2 . Triethylsilane (Et_3SiH , 0.05 mmol) was added at ambient temperature, the reaction mixture was briefly stirred, and then α -methylstyrene (0.05 mmol) was added. The mixture was transferred to an NMR tube and heated at 45 °C for 4 h. The solution was then dried *in vacuo* and re-dissolved in 0.6 mL CDCl_3 affording a colourless solution. Conversions were determined by ^1H NMR

spectroscopy. Mesitylene was added as an internal standard. Product ^1H NMR spectra are consistent with reference spectra.^[9]

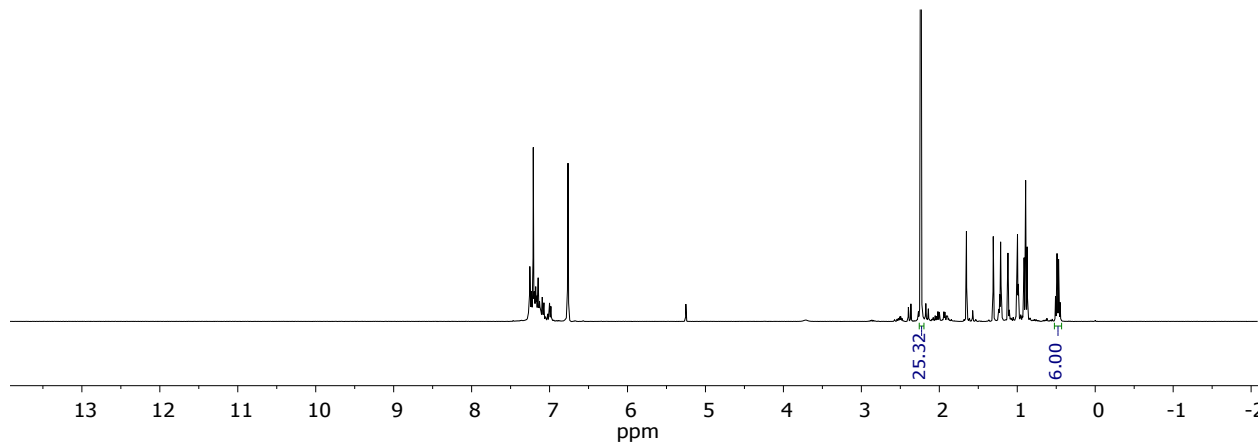


Figure 52. ^1H (CDCl_3) NMR spectrum of catalysis with **1** with mesitylene internal standard (1.6 equiv.).

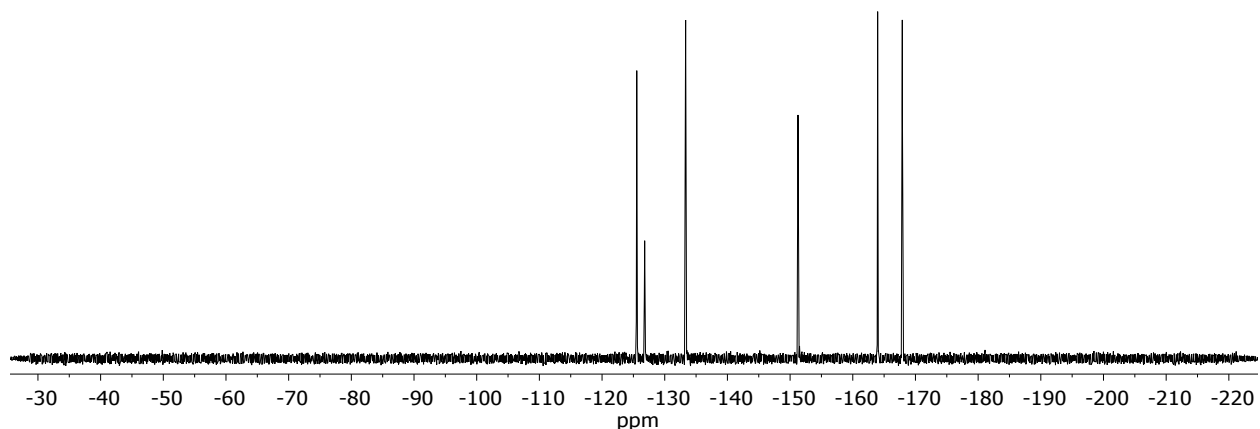


Figure 53. ^{19}F (CH_2Cl_2) NMR spectrum of **1** after catalysis.

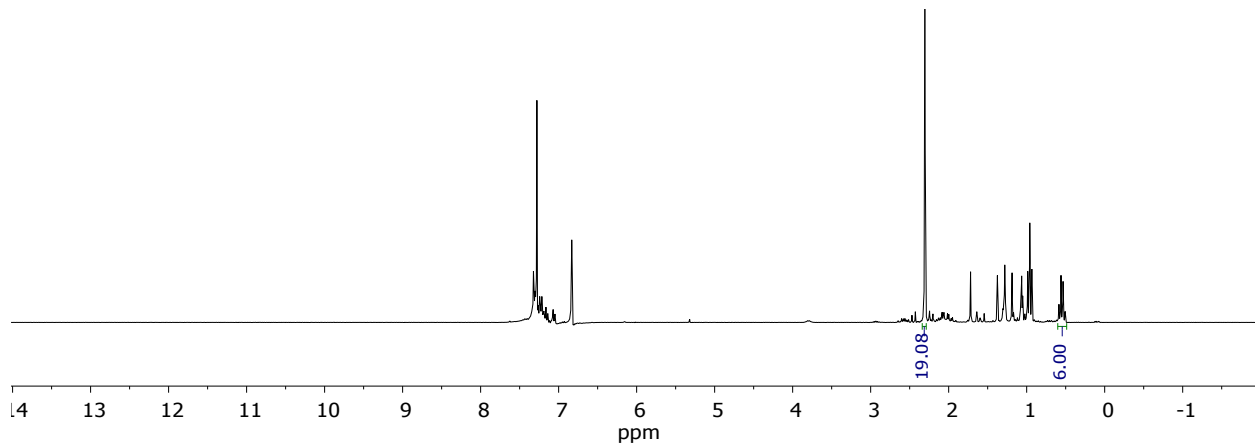


Figure 54. ¹H (CDCl₃) NMR spectrum of catalysis with **2** with mesitylene internal standard (1.6 equiv.).

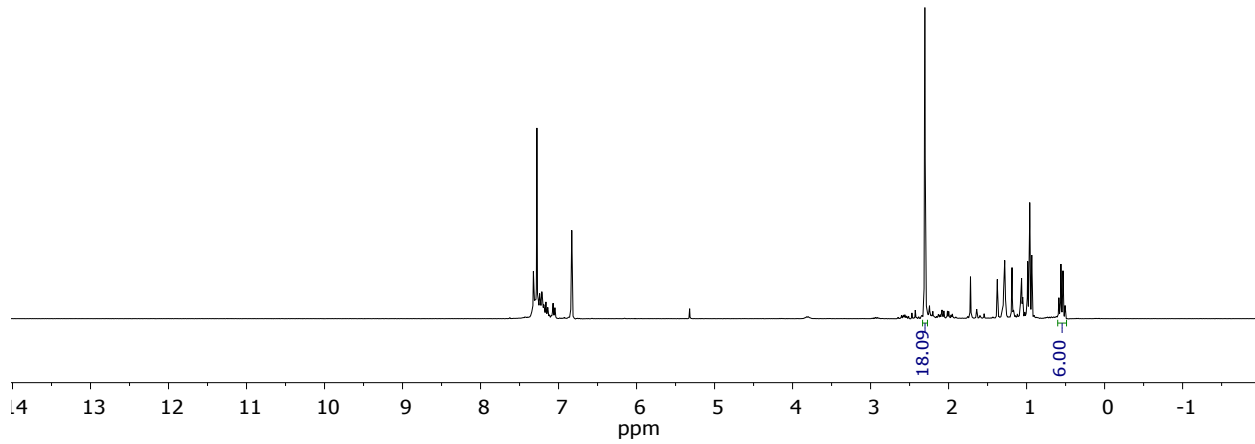


Figure 55. ¹H (CDCl₃) NMR spectrum of catalysis with **3** with mesitylene internal standard (1.6 equiv.).

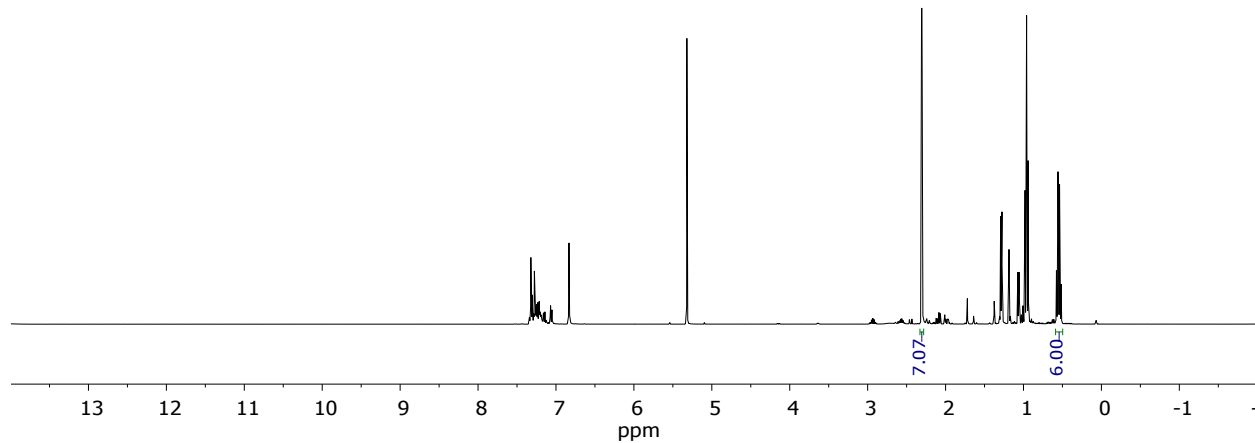


Figure 56. ¹H (CDCl₃) NMR spectrum of catalysis with **4** with mesitylene internal standard (2.4 equiv.).

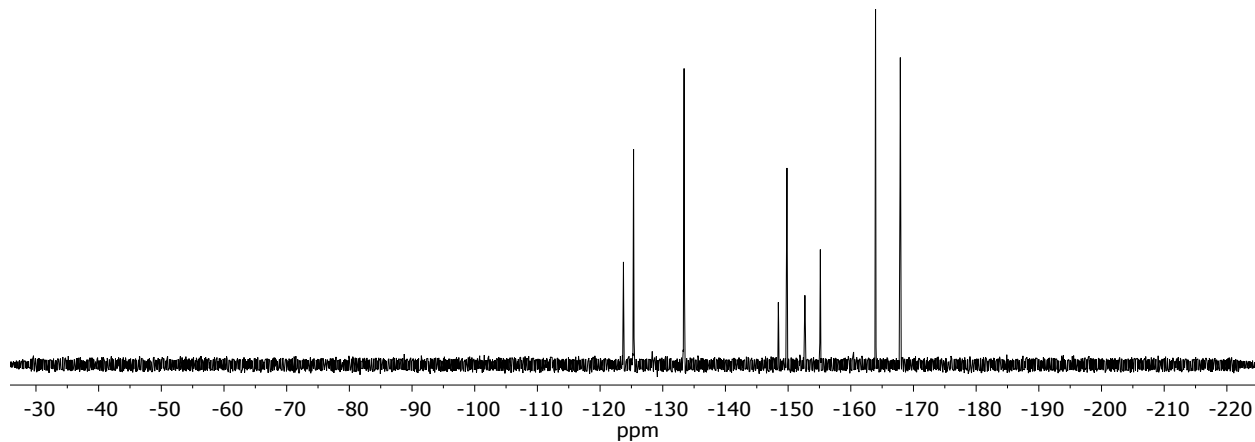
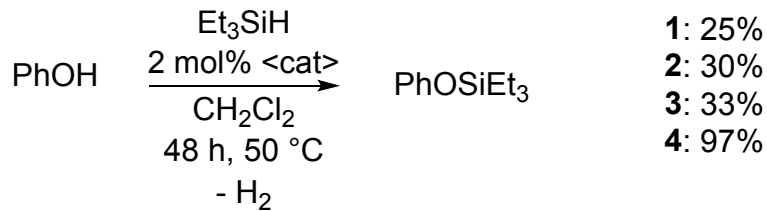


Figure 57. ^{19}F (CH_2Cl_2) NMR spectrum of **4** after catalysis.

5.4 Dehydrocoupling of phenol with Et_3SiH



In a 20 mL vial, a solution of the phosphonium catalyst (2 mol%) was prepared in 0.6 mL CH_2Cl_2 . Triethylsilane (Et_3SiH , 0.05 mmol) was added at ambient temperature, the reaction mixture was briefly stirred, and then added to a vial containing phenol (0.05 mmol). The mixture was transferred to an NMR tube and heated at 50°C for 48 h. The solution was then dried *in vacuo* and re-dissolved in 0.6 mL CDCl_3 affording a colourless solution. Conversions were determined by ^1H NMR spectroscopy. Mesitylene was added as an internal standard. Product ^1H NMR spectra are consistent with reference spectra.^[10]

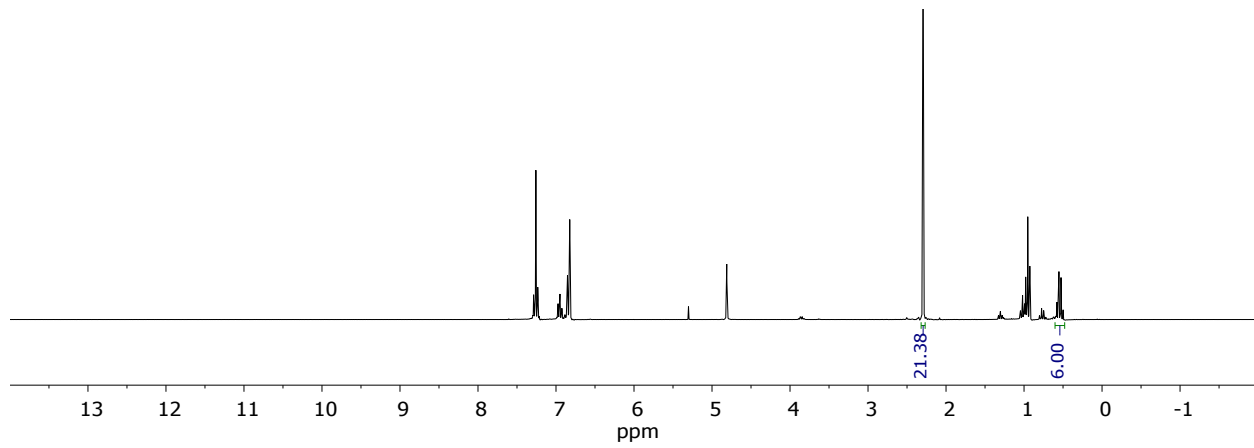


Figure 58. ^1H (CDCl_3) NMR spectrum of catalysis with **1** with mesitylene internal standard (1.5 equiv.).

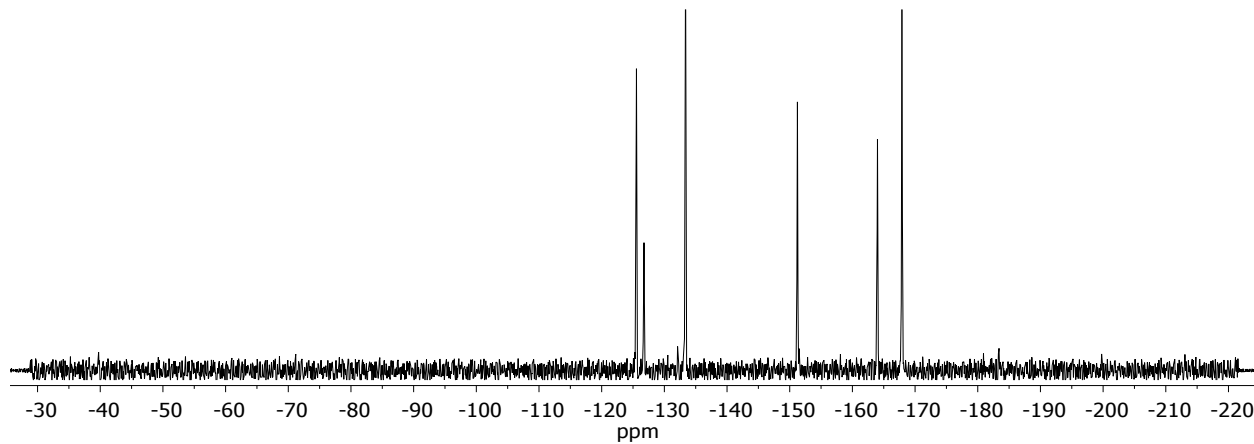


Figure 59. ^{19}F (CH_2Cl_2) NMR spectrum of **1** after catalysis.

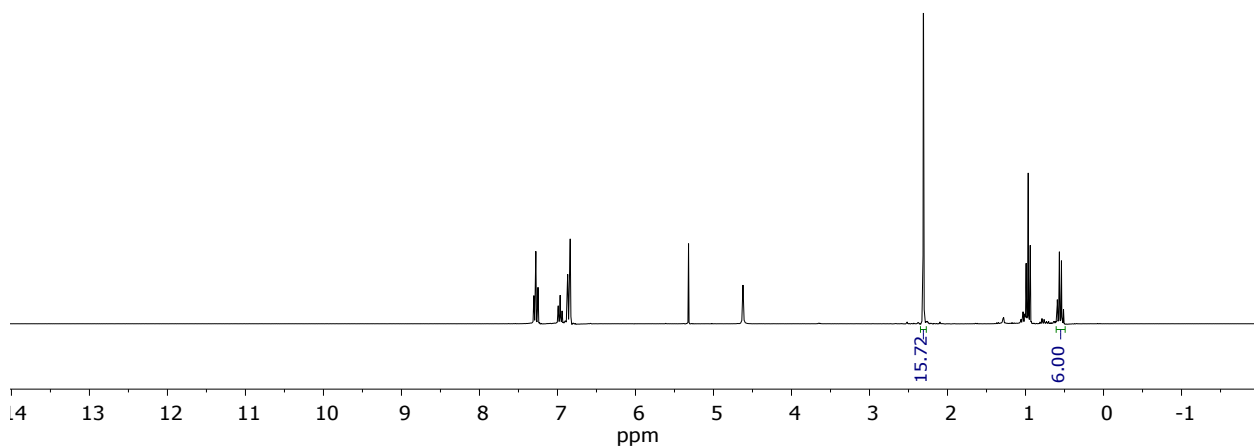


Figure 60. ^1H (CDCl_3) NMR spectrum of catalysis with **2** with mesitylene internal standard (1.6 equiv.).

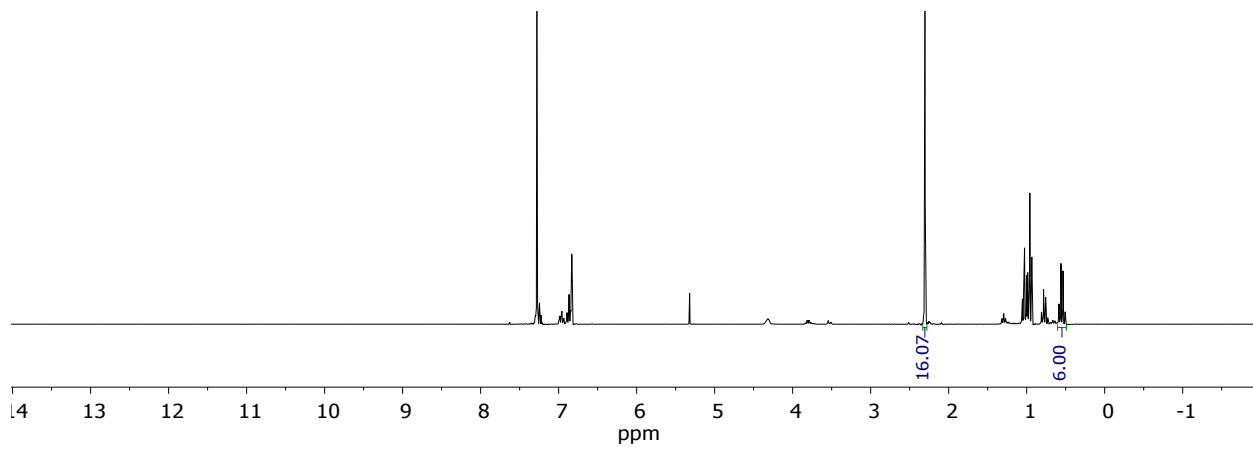


Figure 61. ^1H (CDCl_3) NMR spectrum of catalysis with **3** with mesitylene internal standard (1.5 equiv.).

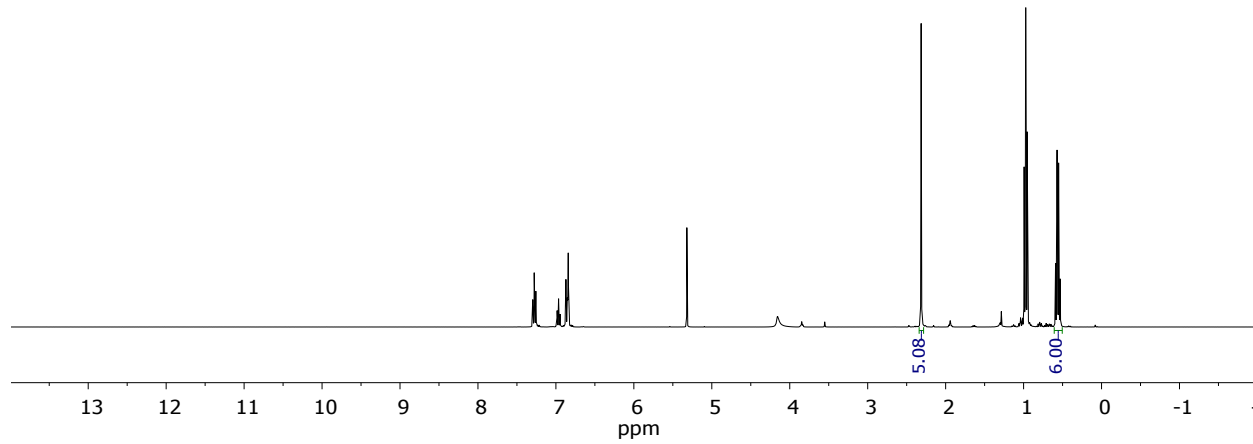


Figure 62. ^1H (CDCl_3) NMR spectrum of catalysis with **4** with mesitylene internal standard (1.8 equiv.).

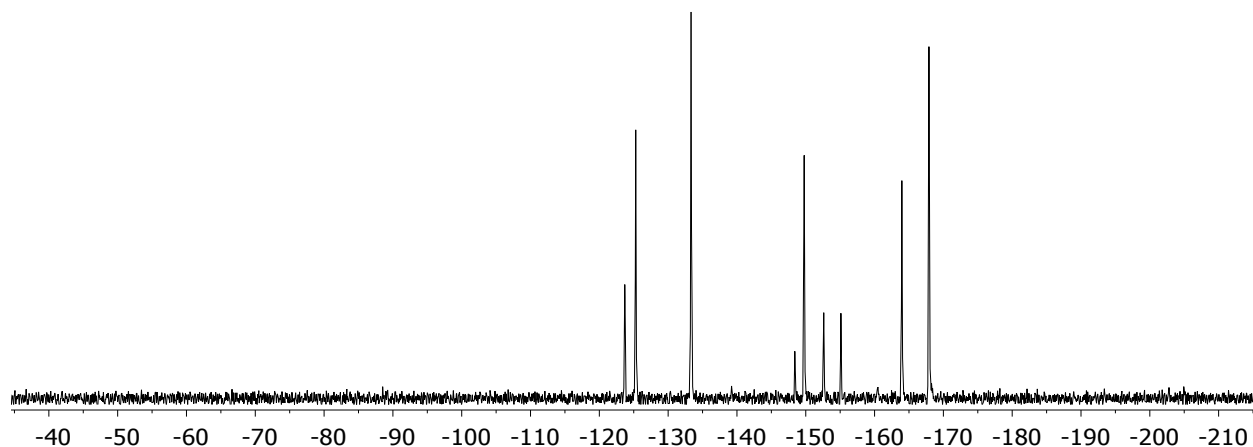
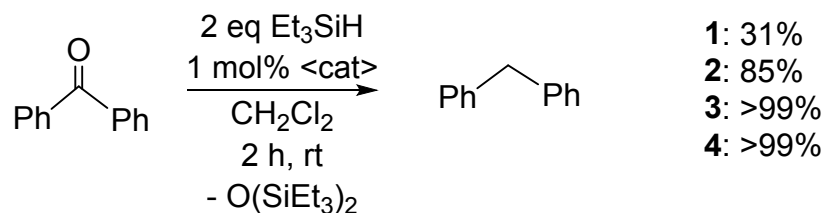


Figure 63. ^{19}F (CH_2Cl_2) NMR spectrum of **4** after catalysis.

5.5 Hydrodeoxygenation of benzophenone



In a 20 mL vial, a solution of the phosphonium catalyst (1 mol%) was prepared in 0.6 mL CH₂Cl₂. Triethylsilane (Et₃SiH, 0.04 mmol) was added at ambient temperature, the reaction was briefly stirred, and then the solution was added to a vial containing benzophenone (0.02 mmol). The reaction mixture was left to stir at ambient temperature for 2 h. The solution was then dried *in vacuo* and re-dissolved in 0.6 mL CDCl₃ affording a colourless solution. Conversions were determined by ¹H NMR spectroscopy. Mesitylene was added as an internal standard. Product ¹H NMR spectra are consistent with reference spectra.^[11]

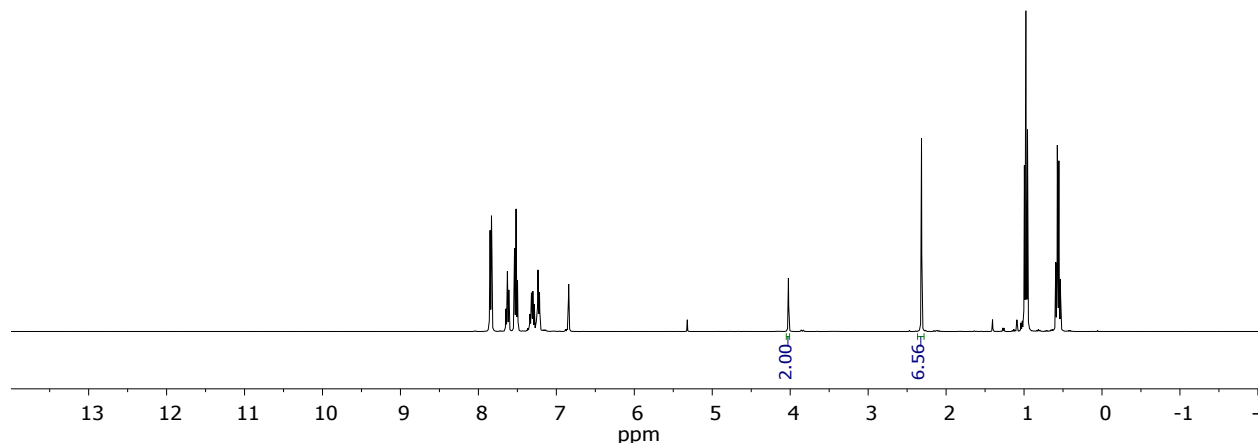


Figure 64. ¹H (CDCl₃) NMR spectrum of catalysis with **1** with mesitylene internal standard (4.6 equiv.).

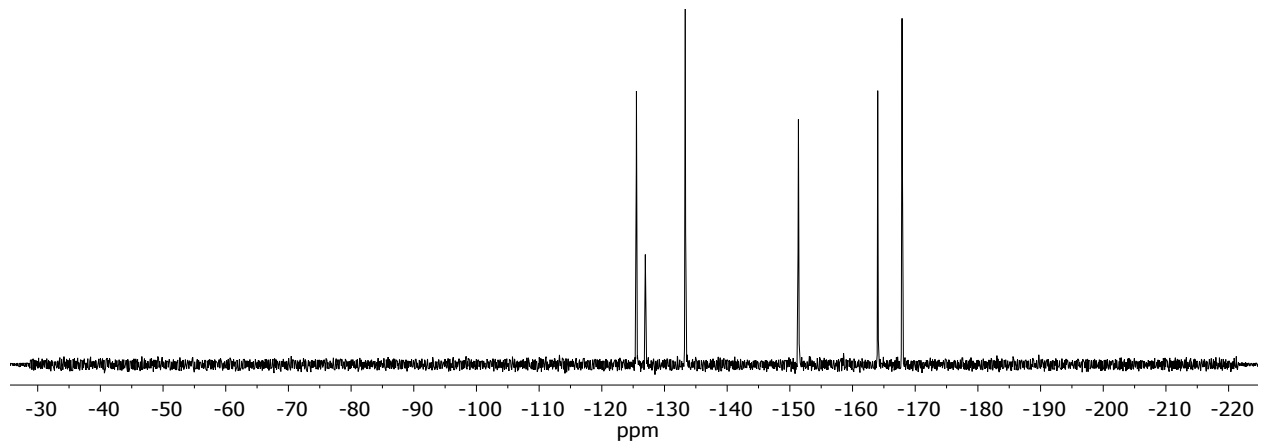


Figure 65. ^{19}F (CH_2Cl_2) NMR spectrum of **1** after catalysis.

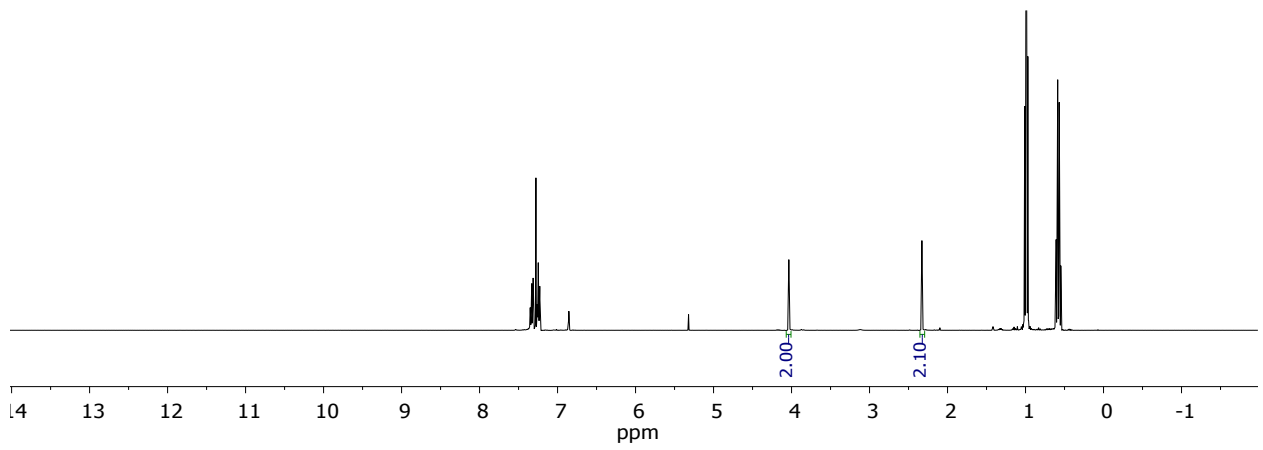


Figure 66. ^1H (CDCl_3) NMR spectrum of catalysis with **2** with mesitylene internal standard (5.0 equiv.).

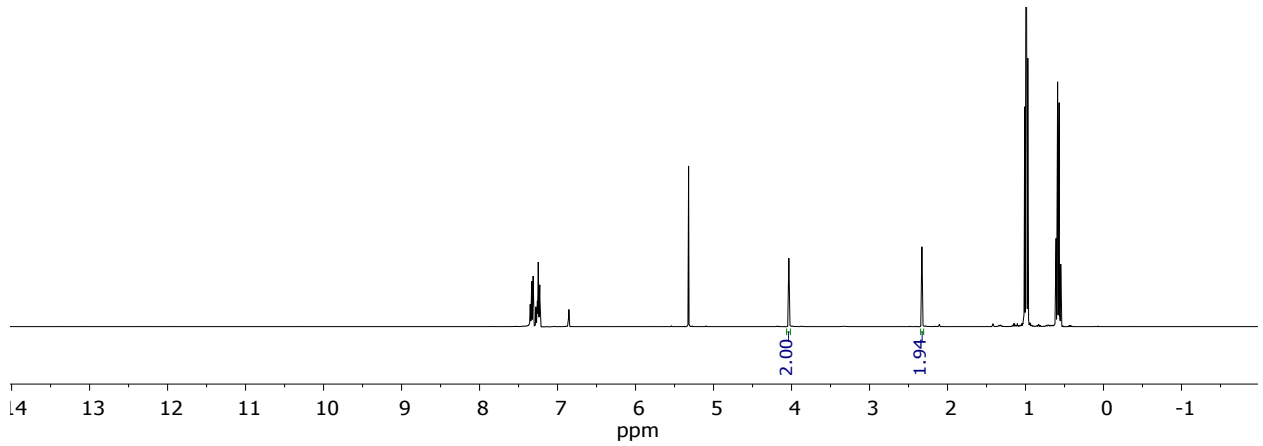


Figure 67. ^1H (CDCl_3) NMR spectrum of catalysis with **3** with mesitylene internal standard (4.5 equiv.).

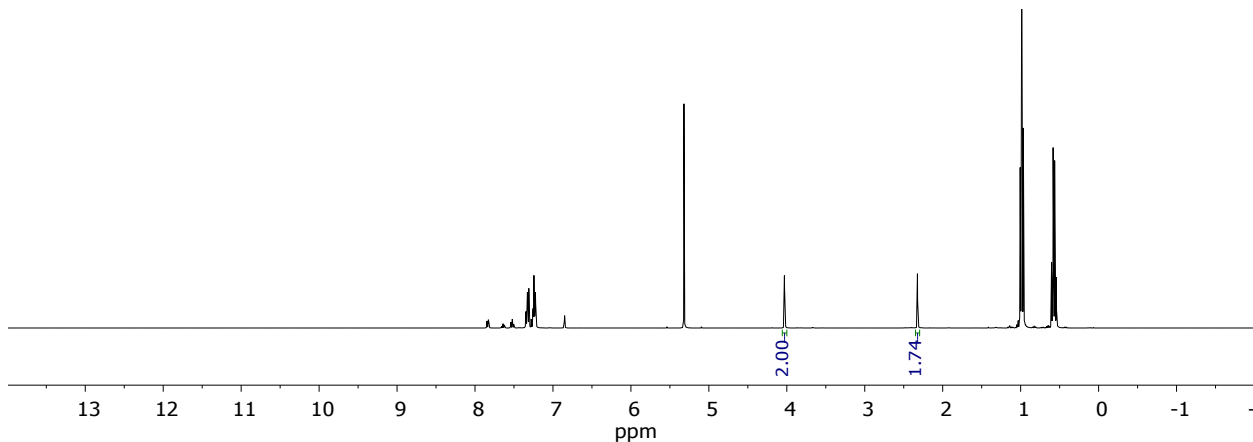


Figure 68. ^1H (CDCl_3) NMR spectrum of catalysis with **4** with mesitylene internal standard (5.1 equiv.).

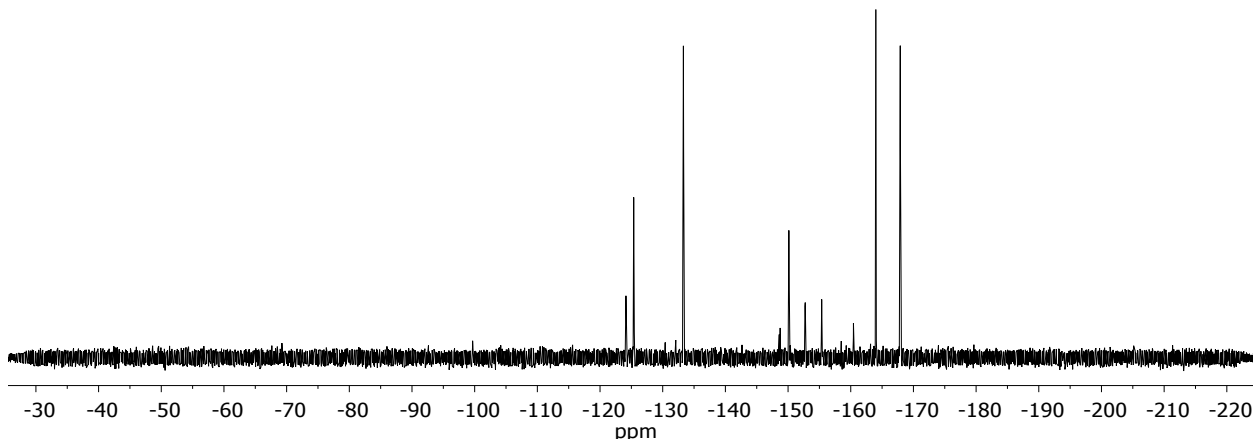


Figure 69. ^{19}F (CH_2Cl_2) NMR spectrum of **4** after catalysis.

6. Computational Details

Electronic structure calculations, including geometry optimization and frequency calculations, were performed using *Gaussian 09* using the range-separated hybrid functional M11 and the polarized triple-zeta basis set def2-TZVP.^[12] Natural bond orbital and natural population analyses were performed on optimized structures using *NBO 6.0*.^[13] X-ray coordinates were used as the starting geometry for geometry optimizations. The Cartesian coordinates of the optimized structures are collected in tables 1-4. The absence of any imaginary frequency with an absolute magnitude greater than 10 cm^{-1} confirmed that each optimized structure was indeed located at

a minimum on its potential energy hypersurface. The electrophilicity index is defined in terms of electronegativity and chemical hardness as in equation 1. [14]

$$\omega = \frac{\chi^2}{2\eta} \quad (1)$$

Using the valence state parabola model, electrophilicity was related to ionization energy (I) and electron affinity (A) according to equation 2.[14] Finally, as approximated in Koopmans' Theorem, the energy of the HOMO was taken as a measure of I and that of the LUMO was taken as a measure of A , as also indicated in equation 2.[15]

$$\omega = \frac{\left(\frac{I+A}{2}\right)^2}{2(I-A)} = \frac{\left(\frac{E_{HOMO} + E_{LUMO}}{2}\right)^2}{2(E_{HOMO} - E_{LUMO})} \quad (2)$$

Table 1. Cartesian coordinates for the optimized structure of **1**.

Center Number	Atomic Number	Atomic Type	Coordinates (Angstroms)		
			X	Y	Z
1	15	0	16.681167	25.951061	4.109852
2	9	0	12.997913	29.712043	6.741338
3	9	0	17.786441	23.460211	3.167411
4	9	0	16.652176	21.512530	1.697652
5	9	0	14.092799	21.786000	0.851792
6	9	0	12.674806	24.000031	1.471518
7	9	0	13.770148	25.935626	2.936679
8	9	0	16.017237	27.479213	1.811007
9	9	0	17.629826	28.583798	-0.073390
10	9	0	20.318208	28.349077	0.180217
11	9	0	21.388960	27.023288	2.272779
12	9	0	19.824026	25.927826	4.123138
13	9	0	16.810068	29.039947	4.157757
14	9	0	15.125381	30.689687	5.388031
15	9	0	12.546981	27.044692	6.846927
16	9	0	14.205445	25.359266	5.582059
17	8	0	17.517760	25.275799	5.239378
18	6	0	13.816361	28.887477	6.128666
19	6	0	14.907090	29.387256	5.434287
20	6	0	15.767341	28.514503	4.796009
21	6	0	15.558142	27.136563	4.822600
22	6	0	16.969237	24.700437	6.422539
23	6	0	16.656236	23.359029	6.414876
24	1	0	16.851501	22.752315	5.535815
25	6	0	16.119637	22.813541	7.571961
26	1	0	15.869136	21.757065	7.599348
27	6	0	15.914292	23.607949	8.690550
28	1	0	15.495291	23.172320	9.592602
29	6	0	15.796543	24.724767	3.158686
30	6	0	16.512460	23.585652	2.788186
31	6	0	15.952035	22.585272	2.023120
32	6	0	14.641612	22.726618	1.586832

33	6	0	13.913961	23.862586	1.908730
34	6	0	14.494020	24.850408	2.680932
35	6	0	17.867150	26.684765	3.011781
36	6	0	17.348595	27.365632	1.912852
37	6	0	18.150315	27.934576	0.953110
38	6	0	19.529591	27.815347	1.086008
39	6	0	20.077164	27.136864	2.162469
40	6	0	19.250787	26.572554	3.121075
41	6	0	13.585700	27.519043	6.182475
42	6	0	14.451925	26.668057	5.533135
43	6	0	16.798245	25.515653	7.521580
44	1	0	17.100328	26.558971	7.483661
45	6	0	16.258747	24.951692	8.668651
46	1	0	16.119349	25.565741	9.553698

Table 2. Cartesian coordinates for the optimized structure of **2**.

Center Number	Atomic Number	Atomic Type	Coordinates (Angstroms)		
			X	Y	Z
1	15	0	0.792555	1.495292	4.093217
2	9	0	0.031945	-0.075217	1.854375
3	9	0	1.565966	-1.214050	-0.076749
4	9	0	3.933281	1.500998	3.985314
5	9	0	4.261422	-0.981433	0.063608
6	9	0	0.902233	-1.590738	4.199516
7	9	0	-1.619368	2.136618	5.651935
8	9	0	1.883939	3.942807	3.035353
9	9	0	-2.167412	1.515083	3.044082
10	9	0	-0.761599	-3.206178	5.501141
11	9	0	5.419474	0.374222	2.090140
12	9	0	-2.837220	-2.187894	6.904170
13	8	0	1.677570	2.191413	5.174330
14	9	0	-3.256412	0.484844	6.988813
15	9	0	-3.300621	3.422909	1.572329
16	6	0	3.318599	0.841860	3.017779
17	6	0	3.512025	-0.432163	0.992565
18	6	0	1.366914	0.034401	1.900672
19	6	0	-0.115072	-1.046149	4.861594
20	9	0	0.714493	5.859868	1.554577
21	6	0	2.128078	-0.550740	0.918109
22	6	0	4.104333	0.261590	2.035093
23	6	0	1.931348	0.731435	2.966799
24	6	0	1.177224	2.838372	6.338095
25	6	0	-1.442537	2.583578	2.728570
26	9	0	-1.882322	5.596723	0.824638
27	6	0	-1.387885	0.824137	5.614234
28	9	0	-0.234025	4.667531	9.655236
29	6	0	-0.119913	2.705988	3.148502
30	6	0	0.593529	3.823001	2.712425
31	6	0	1.018215	2.087526	7.484973
32	1	0	1.288408	1.034882	7.494629
33	6	0	-2.042584	3.556280	1.952107
34	6	0	-0.964979	-1.901304	5.536536
35	6	0	-2.029001	-1.380749	6.256668
36	6	0	-0.309512	0.334268	4.875200
37	6	0	-2.243239	-0.008861	6.300084
38	6	0	0.014627	4.807502	1.940840
39	6	0	0.901065	4.188347	6.275580
40	1	0	1.085984	4.748432	5.363869
41	6	0	0.533191	2.714038	8.621187
42	1	0	0.395971	2.178029	9.554854
43	6	0	-1.314866	4.671406	1.564308
44	6	0	0.417605	4.814429	7.412483
45	1	0	0.190744	5.875748	7.426233
46	6	0	0.235507	4.063031	8.558471

Table 3. Cartesian coordinates for the optimized structure of **3**.

Center Number	Atomic Number	Atomic Type	Coordinates (Angstroms)		
			X	Y	Z
1	15	0	0.757480	1.581835	4.021717
2	9	0	0.008308	-0.096664	1.867778
3	9	0	4.245441	-1.100921	0.147362
4	9	0	-2.718873	-1.902064	7.223801
5	9	0	-1.658387	2.314405	5.533212
6	9	0	1.551201	-1.343051	0.008417
7	9	0	5.394813	0.367721	2.097523
8	9	0	3.900286	1.599246	3.920709
9	9	0	1.843288	4.022900	2.914179
10	9	0	-2.180981	1.550344	2.949772
11	9	0	-3.324853	3.413276	1.425159
12	9	0	0.891213	-1.477976	4.316667
13	9	0	-0.681285	-3.003554	5.830303
14	6	0	1.903373	0.770704	2.938900
15	6	0	3.290441	0.885498	2.989972
16	6	0	4.080086	0.251285	2.044504
17	6	0	3.491918	-0.500596	1.040328
18	6	0	-1.960038	-1.142804	6.467524
19	6	0	-2.209109	0.221979	6.391262
20	9	0	-3.203631	0.756619	7.077475
21	6	0	-1.405258	1.004443	5.594122
22	6	0	-0.345347	0.470040	4.860011
23	6	0	2.108276	-0.624195	0.966484
24	6	0	1.342717	0.015358	1.911148
25	6	0	-0.147017	2.764188	3.036781
26	6	0	0.557430	3.880313	2.584422
27	6	0	-0.027225	4.841260	1.787435
28	9	0	0.663333	5.893384	1.384454
29	6	0	-1.352117	4.681860	1.403948
30	9	0	-1.924134	5.585046	0.641037
31	6	0	-2.070881	3.567070	1.810120
32	6	0	-1.465998	2.617983	2.611369
33	6	0	-0.115398	-0.899980	4.965201
34	6	0	-0.915182	-1.706146	5.751716
35	8	0	1.645098	2.326531	5.078269
36	6	0	1.164018	2.942186	6.247040
37	6	0	0.994531	2.169396	7.383521
38	6	0	0.547575	2.727702	8.559498
39	1	0	0.420769	2.128990	9.455536
40	6	0	0.284069	4.086304	8.556211
41	6	0	0.459100	4.883895	7.439811
42	1	0	0.253084	5.946978	7.502800
43	6	0	0.908378	4.296970	6.269271
44	1	0	1.084971	4.889143	5.375830
45	9	0	-0.149748	4.646490	9.686940
46	9	0	1.269680	0.855144	7.319143

Table 4. Cartesian coordinates for the optimized structure of **4**.

Center Number	Atomic Number	Atomic Type	Coordinates (Angstroms)		
			X	Y	Z
1	9	0	3.724031	17.602442	2.674824
2	9	0	4.910833	19.377468	1.030475

3	9	0	7.491988	19.007127	0.302540
4	9	0	8.880935	16.873413	1.199185
5	9	0	7.724727	15.105098	2.836274
6	6	0	5.707217	16.347479	2.860637
7	6	0	5.004758	17.439392	2.348155
8	6	0	5.593647	18.347245	1.495057
9	6	0	6.916221	18.154744	1.118444
10	6	0	7.630582	17.058779	1.583056
11	6	0	7.022573	16.162605	2.438608
12	15	0	4.804820	15.257690	3.936890
13	8	0	3.984182	16.113792	4.976078
14	9	0	5.009171	18.636952	5.124882
15	9	0	5.781324	19.690302	7.517553
16	9	0	5.624501	18.182206	9.760766
17	9	0	4.704636	15.637392	9.637194
18	9	0	3.921827	14.597971	7.241598
19	6	0	4.438765	16.625278	6.180549
20	6	0	4.366985	15.852177	7.325139
21	6	0	4.766656	16.376758	8.541432
22	6	0	5.238709	17.679189	8.603204
23	6	0	5.317225	18.453851	7.454633
24	6	0	4.918470	17.920371	6.243347
25	9	0	4.627503	12.199922	4.362875
26	9	0	6.252689	10.706079	5.850366
27	9	0	8.343511	11.831483	7.139963
28	9	0	8.821672	14.487731	6.927414
29	9	0	7.214085	16.016184	5.407675
30	6	0	5.881296	14.159098	4.824742
31	6	0	5.653996	12.790732	4.964375
32	6	0	6.483571	12.000653	5.737225
33	6	0	7.556340	12.576470	6.400765
34	6	0	7.801951	13.940419	6.291369
35	6	0	6.966722	14.705923	5.511306
36	9	0	5.403610	13.477616	1.835652
37	9	0	3.739440	12.179896	0.115328
38	9	0	1.061613	12.472491	0.395978
39	9	0	0.044270	14.034870	2.344903
40	9	0	1.658380	15.321701	4.026579
41	6	0	3.582613	14.425688	2.962963
42	6	0	2.202448	14.561361	3.091398
43	6	0	1.352044	13.899428	2.221153
44	6	0	1.872959	13.098520	1.217019
45	6	0	3.248507	12.950130	1.069126
46	6	0	4.074930	13.616864	1.940745

-
- [1] M. Perez, C. B. Caputo, R. Dobrovetsky, D. W. Stephan, *Proceedings of the National Academy of Sciences of the United States of America* **2014**, *111*, 10917-10921.
- [2] C. B. Caputo, L. J. Hounjet, R. Dobrovetsky, D. W. Stephan, *Science* **2013**, *341*, 1374-1377.
- [3] M. Perez, Z.-W. Qu, C. B. Caputo, V. Podgorny, L. J. Hounjet, A. Hansen, R. Dobrovetsky, S. Grimme, D. W. Stephan, *Chem. - Eur. J.* **2015**, *21*, 6491-6500.
- [4] S. F. Rach, E. Herdtweck, F. E. Kühn, *Journal of Organometallic Chemistry* **2011**, *696*, 1817-1823.
- [5] L. Song, J. Hu, J. Wang, X. Liu, Z. Zhen, *Photochemical & Photobiological Sciences* **2008**, *7*, 689-693.
- [6] W. R. Moser, D. W. Slocum, *Homogeneous Transition Metal Catalyzed Reactions*, Vol. 230, American Chemical Society, **1992**.

- [7] H.-B. Sun, B. Li, R. Hua, Y. Yin, *European Journal of Organic Chemistry* **2006**, *2006*, 4231-4236.
- [8] C. B. Caputo, L. J. Hounjet, R. Dobrovetsky, D. W. Stephan, *Science* **2013**, *341*, 1374-1377.
- [9] J. Li, J. Peng, Y. Bai, G. Lai, X. Li, *Journal of Organometallic Chemistry* **2011**, *696*, 2116-2121.
- [10] P. F. Hudrlik, D. K. Minus, *Journal of Organometallic Chemistry* **1996**, *521*, 157-162.
- [11] M. Peña-López, M. Ayán-Varela, L. A. Sarandeses, J. Pérez Sestelo, *Chemistry – A European Journal* **2010**, *16*, 9905-9909.
- [12] aM. J. Frisch, G. W. Trucks, H. B. Schlegel, G. E. Scuseria, M. A. Robb, J. R. Cheeseman, G. Scalmani, V. Barone, B. Mennucci, G. A. Petersson, H. Nakatsuji, M. Caricato, X. Li, H. P. Hratchian, A. F. Izmaylov, J. Bloino, G. Zheng, J. L. Sonnenberg, M. Hada, M. Ehara, K. Toyota, R. Fukuda, J. Hasegawa, M. Ishida, T. Nakajima, Y. Honda, O. Kitao, H. Nakai, T. Vreven, J. A. Montgomery Jr., J. E. Peralta, F. Ogliaro, M. Bearpark, J. J. Heyd, E. Brothers, K. N. Kudin, V. N. Staroverov, T. Keith, R. Kobayashi, J. Normand, K. Raghavachari, A. Rendell, J. C. Burant, S. S. Iyengar, J. Tomasi, M. Cossi, N. Rega, J. M. Millam, M. Klene, J. E. Knox, J. B. Cross, V. Bakken, C. Adamo, J. Jaramillo, R. Gomperts, R. E. Stratmann, O. Yazyev, A. J. Austin, R. Cammi, C. Pomelli, J. W. Ochterski, R. L. Martin, K. Morokuma, V. G. Zakrzewski, G. A. Voth, P. Salvador, J. J. Dannenberg, S. Dapprich, A. D. Daniels, O. Farkas, J. B. Foresman, J. V. Ortiz, J. Cioslowski, D. J. Fox, Gaussian, Inc., Wallingford, CT, **2013**; bR. Peverati, D. G. Truhlar, *Journal of Physical Chemistry Letters* **2011**, *2*, 2810-2817; cF. Weigend, R. Ahlrichs, *Physical Chemistry Chemical Physics* **2005**, *7*, 3297-3305.
- [13] E. D. Glendening, J. K. Badenhoop, A. E. Reed, J. E. Carpenter, J. A. Bohmann, C. M. Morales, C. R. Landis, F. Weinhold, Theoretical Chemistry Institute, University of Wisconsin, Madison, WI, **2013**.
- [14] R. G. Parr, L. v. Szentpály, S. Liu, *Journal of the American Chemical Society* **1999**, *121*, 1922-1924.
- [15] P. K. Chattaraj, U. Sarkar, D. R. Roy, *Chemical Reviews* **2006**, *106*, 2065-2091.